Application of Cutting-Edge 3D Seismic Attribute Technology to the Assessment of Geological Reservoirs for CO2 Sequestration

Type of Report:	Progress
Frequency of Report:	Quarterly
Reporting Period:	January 1, 2009 – March 31, 2009
DOE Award Number:	DE-FG26-06NT42734 [University Coal Research] (UH budget G091836)
Submitting Organizations:	Department of Earth and Atmospheric Sciences Reservoir Quantification Lab University of Houston Houston, Texas 77204-5505
Preparers:	Prof. Christopher Liner - P.I Dr. Jianjun (June) Zeng Dr. Po Geng Heather King Phone: 713-743-919 Fax: 713-748-7906

CONTENTS

Executive Summary

This report presents six major areas of progress in geology, geophysics, formation property modeling, and reservoir simulation for the Dickman Field CO_2 sequestration project occurring January 1st to March 31st of 2009. The research workflow is characterized and progress has been enhanced by intensive inter-disciplinary collaboration between members with different areas of expertise.

Major accomplishments in geology include (1) a detailed study on regional geology, lithology and depositional environments of the Fort Scott Limestone Formation (2) update of Petrel stratigraphic/structure/property model from M2 version (discussed in Dec. 2008 report) to M3 version to include more geological integrity. The M3 model serves as an initial input data set to the CMG Grid Builder.

Major accomplishments in geophysics include (1) a quantitative analysis on the vertical resolution and detection limit of seismic data taking the Fort Scott Formation as an example (2) an optimized parameter set in the computation of seismic attributes, especially negative and positive curvature, for a better visualization of lineations of geological interest in the merged survey area.

Major accomplishments in reservoir simulation include (1) a preliminary Dickman Field simulation grid using CMG Grid Builder donated by Computer Modeling Group Ltd. (2) a pre-simulation data assessment, including well production, DST, and core analysis data, as a starting point for history matching and assessment of reservoir fluid and rock properties.

Activities in Quarter

Geology

Activities in geology include two major aspects. The first aspect is a detailed study on the Pennsylvanian Fort Scott Limestone including regional stratigraphy, lithology and depositional environments. The second aspect is the third cycle of Petrel modeling on the shallow reservoirs and deep saline aquifer, containing the sub-division of lithozones within targeted Mississippian strata in the stratigraphic model, a refined fault framework in the structure grid, and the computation of zone-averaged formation properties in the property model. As a result, the M2 model grid (discussed in Dec. 31, 2008 report) was updated to the M3 model. The following discussions in geology refer to the general geological column shown in Fig. 1, an updated version of the one shown in the June 30 2008 report. Furthermore, composite logs for four wells were produced using SMT KINGDOM Software, to detail the geological information from the top of the Fort Scott Formation down to the Gilmore City Formation. Fig. 2 shows an example composite log for the Elmore 3 well.

Fort Scott Seal Integrity

Fort Scott Limestone is the lowest formation in the Marmaton Group, stratigraphically overlaying the Cherokee Group (Figs. 1, 2). A black shale bed below the Fort Scott Limestone marks the uppermost part of the Cherokee Group, which is uniformly identified from the GR logs in the Dickman survey area (Fig. 3). The top of the Fort Scott Limestone is taken as the hanging datum of the stratigraphic model for flow simulation of Dickman study. The thickness of the upper Fort Scott limestone ranges from 25 to 30 ft in the survey area (Fig. 3). The Post-Mississippian stratigraphic units below the Fort Scott formation contain one of the targeted CO_2 sequestration reservoirs (Lower Cherokee Sandstone, LCS) and the regional seal beds for both clastics and Mississippian carbonate reservoirs.

Lithology: the Marmaton Group containing the Fort Scott Limestone has been described based on outcrop descriptions from a large belt (10 to 25 miles in width) of outcrops along the Kansas-Missouri boundary as shown in Fig. 4 (Moore, 1949). For this discussion, the formation definitions and descriptions outlined in Moore (1949), which are generally accepted throughout Kansas and have been adapted by Zeller (1968), and Merriam (1963), will be followed.

Moore (1949) defines the Fort Scott Limestone formation as being composed of two limestone members separated by a shale member. The total formation thickness ranges from 13-145 feet with an average of about 30 feet throughout Kansas (Merriam,1963). The upper member is the Higginsville Limestone which is light to dark gray with a medium-grained crystalline texture and a brecciated appearance. Irregular wavy beds and stems of fusulinides and large crinoids are found throughout the member with the upper portion mostly made up of a coral called Chaetetes. The middle member is the Little Osage Shale which is a grey to black fissle shale with an interbedded layer of coal in the lower section and a very thin limestone in the middle. Both are less than 1 foot in thickness in Kansas. Fossils are scarce throughout the middle member. The lower

member is more variable depending on location, but can generally be described by an upper portion that is light gray with a coarse crystalline texture and irregular bedding and a lower portion that is tan, brownish, or dark gray fossiliferous limestone with thicker and more regular bedding. The upper portion contains Chaetets and fusulines while the lower portion commonly contains mollusks and conchoidal fractures.

Depositional Environment: the Marmaton Group, as well as the Cherokee Group stratigraphically below it, are dominantly composed of marine and non-marine deposits indicative of numerous advances and retreats of a shallow sea. Throughout both groups, the sequences approximately follow the following order, taken directly from Merriam (1963): "(1) non-marine sandstone, commonly uneven at the base, occupying channels cut in subjacent rocks, (2) sandy, silty, and clayey shale, unfossiliferous or containing land plant remains, (3) underclay, (4) coal, (5) black platy shale containing conodonts, and commonly bearing small spheroidal phosphatic concretions, (6) gray to brownish clayey or calcareous shale, or limestone containing a varied assemblage of marine invertebrates." The fossiliferous limestone portions of the Fort Scott Limestone (6) are indicative of the latest stage of an advance of a shallow sea while the intervening shale portion would indicate slight retreats of the sea before further advancement allowing deposition of the overlying upper units of the Fort Scott. While sequences often lack certain lithologies from the above description, the order of appearances is generally followed throughout the Marmaton group (including formations extending above the Fort Scott Limestone) and Cherokee group below.

The coal-bearing shale beds within the Fort Scott and Cherokee Group are considered as seals for the oil producing zones in the Cherokee Group and in strata below, including the simulation target of this study. Therefore the above information for Fort Scott Limestone provided a base to start accessing the seal integrity for the flow simulation.

Petrel Modeling

The third cycle of the Petrel modeling (M3 model) is improved in several ways. The new lithozone divisions in the Mississippian carbonate reservoir and deep saline aquifer for deriving zone-average reservoir properties. The fault/fracture interpretation has been updated based on evidence independent of seismic volume attributes for setting constraints in flow simulation mode. There are now better up-scaling and correction of log porosity based on lithozones, to be assigned to seed cells in the modeling grid. . We have also done data analysis on relationships between core porosity and permeability, between core porosity and log porosity, and between the impedance and neutron porosity. The first two relationships are used for computing permeability from porosity logs, and the last for guiding the propagation of permeability in property modeling. The M3 model also incorporates geological data collected from additional fields partially covered by the merged seismic area, such as the Dickman North, Kelman North and Aldrich Northeast Fields (Fig. 5). The precision of time-depth conversion for the M3 grid was improved by a refined velocity model based on localized time-depth ratio (TDR) curves. The M3 model served as an initial input data set to the CMG Grid Builder for flow simulation. The following paragraphs give insights into accomplishments from activities in building the M3 model.

Stratigraphic Modeling: Four litho-zones below the Mississippian Unconformity were identified based on available well tops from 27 wells, log interpretations (details in June 30, 2008 report), and core studies from similar stratigraphic units in nearby oil-production fields. These lithozones are: Salem Limestone and Warsaw Limestone of Upper Mississippian Age, and the upper and lower Osage lithozones of Lower Mississippian Age (Figs. 1, 6).

The Salem Limestone conformably overlies the Warsaw Limestone. Subject to strong erosion during the Post-Mississippian uplift, the Salem is mostly missing with a residual thickness up to 30 feet (GIS of KGS, 2009). In the survey area, the Salem Limestone is poorly identified in only a few wells mostly to the north of the survey area, including Dickman 1, 4, Phelps1a, and Telley3. The residual Salem is likely located on buried highs of Karst geomorphology. The lithology of the Salem Limestone in northeastern Kansas consists mainly of non-cherty or sparsely cherty saccharoidal to silty dolomite interstratified with non-cherty calcarenite. It also contains a small amount of microfossiliferous chert that resembles those in the underlaying Warsaw Limestone (Carr, et. al., 1999). It is a part of the carbonate reservoir in Dickman Field.

The Warsaw Limestone is seemingly conformable on the underlying strata in western Kansas (Goebel, 1966) including the survey area. The top was partially eroded during the Post-Mississippian uplift. The thickness ranges from 0 to over 60 ft in the survey area. The Warsaw Limestone consists mainly of semigranular limestone interlaminated with saccharoidal dolomite, including relatively large amounts of distinctive, gray, mottled, opaque, microfossiliferous chert. Glauconite occurs in the lower part. Insoluble residues of some dolomites contain masses of sponge spicules. A part of Warsaw is the main carbonate reservoir, such as in Humphrey 3-18 and Dickman 2, and a part of it makes up the saline aquifer around Dickman Field (5-6 feet below the OWC) and Sidebottom 6 area.

The Osagian overlays on the Kinderhookian Stage at an angular unconformity (Goebel, 1966) corresponding to the Gilmore City top in this project (GCU, Fig. 1). Well logs show a sharp change in lithology (Fig. 6) across the GCU, indicative of this unconformity. The angular pattern of this unconformity has not been resolved from the seismic data, not surprising given the less than 0.15% difference in dips between Warsaw/Osage and the GCU (computed from State Well Tops Stratigraphic Viewer, GIS of KGS). The geomorphic anomalies shown by amplitude and curvature time slices through the GCU, interpreted as sinkholes formed during early karst development, also suggest sub-areal exposure and erosion on the GCU. The Osagian Stage seen in the studied area belongs to the younger part of the Osage Stage as the older Osagian is missing (Carr et. al., 1999). The thickness of the Upper Osage in the survey area ranges from 55 to 81 ft and makes up the deep Saline aquifer.

In the M3 stratigraphic model, the Upper Osage is further divided into two lithozones, as UO1 and UO2 (Figs. 1, 6), correlated to the two Upper Osage lithozones seen in cores of the Schaben Field (which produces from upper Osage) about 50 mile southeast to the Dickman Field. This correlation is possible because the two fields have very similar structural and stratigraphy. This correlation is necessary because the Upper Osage deep saline aquifer has little well penetration in the Dickman field survey area while the Upper Osage oil reservoir in Schaben Field has intensive well-penetration and core studies. According to the core study in Schaben Field, “an internal unconformity,

apparently a sub-aerial exposure event", termed as an "M1 Surface", separates the Upper Osagian into upper and lower zones, with different sedimentary facies and therefore different reservoir properties (Franseen et. al., 1998, Carr et. al., 1999). The upper lithozone, termed as "M1 unit and above", about 45-60 feet thick, is made of "sponge spicule-rich facies and silicified original evaporite minerals (SWP facies)", typical of ramp carbonates including restricted evaporitive ramp, lagoon, or supratidal environments. It intersects the Mississippian Unconformity to become a prolific production zone. While the lower lithozone below M1 Surface, contains mainly "normal to somewhat restricted marine strata characterized by an abundance of echinoderm-rich facies with poorer internal conductivity" (Franseen, 2006, Carr et. al., 1999). The UO1 and UO2 lithozones seen in the Dickman stratigraphic column (Figs 1, 6) are correlated to lithozones of "M1 unit and above" and "below M1 Surface", respectively. The thickness is around 40-45 ft for the former, and around 30 ft for the latter. Data on the Upper Osagian in the Schaben Field core study helped improve our understanding of the lithology and properties of the deep saline reservoir and to fill the gap between data available and data needed for the flow simulation in the deep saline aquifer.

The above subdivision of the strata below the Mississippian Unconformity into four lithozones allows up-scaling and correction of zone-averaged reservoir properties based on lithology for the property modeling. This will be discussed in the "Property Modeling" section.

Fault/fracture Modeling: Efforts were made to resolve a conflict resulting from studies of different volumetric seismic attributes. As stated in Dec. 31, 2008 report, the previous study on seismic curvatures, 25 ms below the Mississippian Unconformity in the north part of the survey, suggested a nearly vertical fault/fracture network (Nissen et. al, 2004, 2006, their Fig.15), while results from Petrel ANT attribute modeling, for all target lithozones of the entire survey area, revealed more low-angle or near-horizontal planes of discontinuity (Fig. 21, Dec.31, 2008 report). Moreover, the ANT modeling did not show significant NW-oriented lineations that are interpreted as open fractures by the curvature study. Whether such a vertical fault/fracture framework exists in the area, and if so, its influence on the fluid flow, is critical in setting constraints in the M3 grid for CMG flow simulation.

During this reporting period, the curvature attributes were recalculated using optimized parameter sets (details in the following Geophysics section) for the entire survey area. The resulting time slices were compared with time slices from two versions of ANT volumes in Petrel, to visualize similarities and differences in patterns of lineations and other types of discontinuities. In addition, evidence independent of seismic attributes were collected to better understand these similarities and differences. The collected data are at varying geological scales including: (1) the Pre- and Post-Mississippian structure deformation history; (2) the ideal types and patterns of lineations/discontinuities associated with structural deformation of carbonate strata; (3) possible indicators of fractured zones from well logs; and (4) structural-fractures identified from photos of Osage cores in the analog field.

Regional structure deformation history provides a primary control on the stress field of carbonate strata in the Dickman field. The survey area is on the Southwest flank of the northwest-southeast trending Central Kansas Uplift (CKU) as shown in Fig. 7. The CKU was created largely by geologic deformation in late Mississippian to early

Pennsylvanian time (Merriam, 1963; Blakely, 2004). This deformation is likely associated with the plate convergence along the Ouachita Mountains orogenic belt in Arkansas (Newell et al., 1989) when North America was welded to Gondwanaland from the southeast. This event is considered the latest major structure deformation seemingly inherited from old fractures bounding the pre-Cambrian basement in Kansas (Gerhard, 2004). Lineations in Fig. 7 give a general pattern of these old bounding faults/fractures that were probably reactivated during the Post-Mississippian uplift. The linear pattern of oil drilling (green lines) along the southwest side of CKU has both NE (north) and SW (south) orientations. Drainage patterns (red) developed along zones of weakness show similar orientations. Although the behavior of the motion along these faults/fractures is unclear, the above regional structural history favors the formation of a structure framework with NW- and NE-oriented faulting and fracturing in the study area. In Fig. 7, a secondary northeast-trending anticline structure (blue) exists to the southwest of the survey area with an axis almost perpendicular to the axis of CKU. Structures like this on the SE flank of CKU may have influence on the strata deformation in the studied area, as suggested by the observation on top maps of Ness County (State Well Top Stratigraphic Viewer, GIS of KGS). Mississippian strata in Ness County dip to the southwest, slightly diverging from the regional southeast dip orientation of Mississippian on the SE flank of CKU. The angle of dip ranges from less than 1.5/1000 for the younger Warsaw Limestone, to less than 3/1000 for the older Osagian and GCU as computed form the top maps. This may be attributed to the influence of secondary structures perpendicular to the CKU. Therefore, more undiscovered NE or NW oriented fractures associated with secondary structures along the SE flank of the CKU may be expected.

Simulation on carbonate deformation gives an ideal pattern of lineations related to the regional stress field. This improves our understanding of the different types of faults, fractures, and discontinuities and the motion along them. Fig. 8 shows results from a simplified 3D simulation model with various types of discontinuities (Fig. 5-7, OuYang, 1994). At least three types of discontinuities may be associated with the simple folding and uplifting of carbonate strata. First, longitudinal and transverse fractures, the former are parallel to the structural axis and mostly open and the latter are perpendicular to the structural axis and mostly closed. Second, conjugate diagonal fractures, around +/- 45 degree to the structural axis with the intersections being points of weakness for dissolution when exposed. Third, vertical (to bedding plane) and horizontal (to bedding plane) stylolites resulting from pressure dissolution, commonly perpendicular to the direction of normal stresses. Both types one and two fractures result from brittle deformation of carbonates, mostly penetrating the entire strata at high angles. Several NE-oriented vertical discontinuities, revealed by both ANT and curvature analysis in the survey area, may be related to types one and two structures, serving as vertical barriers or conduits to the flow simulation grid. Type three fractures are confined within stratigraphic units and may be perpendicular or parallel to the bedding planes and probably dissolution-prone when exposed. Some low-angle or near-parallel planes of discontinuities revealed by Petrel ANT modeling may be related to type three discontinuities. They may act as indicators for the reservoir conductivity to guide the property propagation within the lithozones. Some other features revealed by ANT and curvature analysis may be attributed to karst geomorphology. The first being sinkhole features most likely at junctions of fractures during the early stage of karst development

(as shown by seismic time slices at the Gilmore City unconformity horizon) and the second being collapsed underground caves or tunnels during the later stage of karst development (as shown by slices at the Mississippian Horizon). A present day analog of sinkhole geomorphology with a block diagram showing the development of Karst features within the strata is shown in Fig. 9.

Log indicators on fractured zones in carbonate strata provide more solid evidence of fractures but at a very local scale. They include gamma log spikes, sonic log spikes, positive deviations between deep and shallow resistivity readings (RLD and RLS). Gamma and sonic spikes in carbonate lithozones may indicate mud-filled fractures. Pure limestone and dolomite have very low GR (0-5 and 0-20, respectively) and are acoustically fast (with DT around 40ms). Fractures allow the ground water flow to carry some muddy infill with much higher GR and acoustic slowness. Resistivity logs reading deeper in the formation (RLD) and reading near-hole conditions (RLS) reflect differences in salinities of formation water and drilling fluid. In the Upper Mississippian saline aquifer, the formation water salinity is much higher (water density ranging from 1.023 to 1.035), with much lower formation water resistivity from 0.14 to 0.27 at 73^{o} F (from the KGS Brine Analysis database) than that of the drilling fluid (with RMF = 0.9 at 73^{o} F (from the Humphrey 4-18 log header). In dense carbonates with very narrow flushed zone the higher salinity of formation water results in RLD < RLS. Fractured zones allow a deeper invasion of drilling fluid into the surrounding saline aquifer, narrowing or even reversing the differences between the RLD and RLS (i.e., RLD>=RLS). Positive and highly variable RLD-RLS with depth may be taken as an indicator for fractured zones in carbonates.

Although the GR, DT and RLD>RLS may not align exactly in depth since most fractures are not vertical to the borehole trace, together they provide estimates on pay zones and fractured zones as shown in Fig. 10, showing the GR, DT and RLD-RLS logs for the Humphrey 4-18 and Sidebottom 6 wells. The zones with very high ILD but highly varying RLD-RLS values in well Humphrey 4-18 (Fig. 10c) reflect the Warsaw Limestone pay zone. Oil in formation has very high resistivity (RLD), but the RLD-RLS values change significantly through depth with negative and positive peaks. The positive peaks reflect the high resistivity of oil relative to drilling fluid while zero and negative peaks may reflect the invasion of drilling fluid into the oil-bearing formation via fractures. Overall, the log indicators provide only faint evidence for a few possible fractured zones in the deep saline aquifer where the RLD-RLS values from zero to positive are associated with GR and DT spikes kicking to the right (blue arrows, Fig. 10). The deep saline aquifer in the two wells is relatively tight compared to the shallower reservoir.

Core photos give direct evidence of fractures and their properties at a micro-scale. Calcite filled fractures are commonly associated with open fractures while clay-filled fractures are indicative of closed ones. The study of Osage core photos in the Schaben Field (Fig. 11, from Fig. 10 of Franseen, 2006) reveal some brecciation and fracturing but the fractures mostly were attributed to non-structural origins. Non-structural fractures and brecciation were formed by early differential compaction between silicified areas and the surrounding matrix, early subaerial exposure of M1 surface (shrinkage during dolomization), post-Mississippian subaerial exposure (karst development), and late burial compaction (Franseen et. al, 1998, Carr et. al., 1999). The extension of these non-structural fractures is within individual stratigraphic zones. In core photos, a few

siliclastic-filled fractures and layers do exist while observation of several generations of crosscutting fractures were considered as brittle deformation associated with post-depositional uplifting (Franseen, 2006). In general, however, cores revealed only faint evidence for structure-related fracturing. The depositional facies and early diagenetic events were dominant controls for reservoir characteristics (Franseen, 2006, Carr et. al., 1999). Low quality of core photos increased the difficulty in recognizing structural-related fractures that penetrate all lithozones.

Based on the above fracture study from regional to core scales, the fault model from ANT extraction is simplified to exclude linear features within stratigraphic units and planes with dip angles near-parallel to the strata. This significantly simplified the flow simulation grid by minimizing the number of modeling segments. On the other hand, the fault modeling study has so far not provided enough positive evidence for a NW-oriented open fracture system.

In order to add the above results from stratigraphic and structural modeling to the gridded framework, a log-seismic overlay using all available wells was constructed, shown in Fig. 12. The gridding of newly added horizons into surfaces is controlled by the two-way time values of well tops from seed wells (Fig. 2 in Dec. 31, 2008 report). The resulting surfaces were added to the 3D gridded structure model with the faults intersecting the strata, as shown in Fig. The gridded structure model integrates as much as possible the available information from multiple sources into a single framework for property computation, including 3D variation of thickness of lithozones (color bends) on arbitrary intersections, gamma and neutron logs at 17 well locations, core porosity and permeability for Mississippian carbonate pay zones at a few well traces, horizon-fault intersections where the lithozones are cut by major faults, and cross-cutting relationships between lithozones. For instance, the Lower Cherokee sands filling the low areas on the Mississippian Unconformity is seen to thin northward from the Staiwalt 1 well through the Phelps1a well where the pay zone is from the LCS and completely missing around the Dickman 6 well area where the pay zone is from Salem and Warsaw (most likely on top of buried karst highs).

The above stratigraphic and fault framework was converted to the depth domain to make it readable by the CMG Grid Builder. The lateral continuity of the M3 layering model is improved significantly compared to the M2 model which was influenced by significant lateral variation in seismic velocity (Fig. 25, Dec. 31, 2008 report). These improvements were obtained through a revised velocity model using 23 localized time-depth-ratio (TDR) curves, and the zone-averaged velocity computed from sonic logs in five wells (Fig. 14). The oil water contact was added to the M3 model for quality control and for volumetric computation (Fig. 15). This framework is being input into the CMG flow simulator. Quality control processes still revealed misties remaining in the M3 model, which will be a task for the next reporting period.

Property Modeling: The property modeling tool in Petrel distributes the porosity and permeability from seed cells (well data) to the entire grid. The porosity and permeability values must be calibrated from log and core data and inserted into seed cells. During this reporting period, the zone-averaged log properties, including neutron porosity (NPHI) from 17 wells and density porosity (DPOR) and sonic porosity (SPOR) from two wells were computed using newly divided lithozones. Gamma ray (GR) logs are also up-scaled by lithozones as a factor for lithology corrections. Fig. 16 shows an example

output of zone-averaged NPHI values over the entire target strata between the Mississippian and Gilmore City unconformities. Maps for individual lithozones will be available after resolving a software issue in mismatching property values with zone names. The resulting zone-averaged porosity for limestone will be corrected based on contents of dolomite in lithozones before being assigned to seed cells.

Reservoir permeability is another critical variable for flow simulation. In the study area, it was measured on cores covering a small portion of Salem/Warsaw Limestone from seven wells around the Dickman Field area. For the majority of wells and lithozones with no core coverage, the permeability has to be estimated from porosity values. This estimation is based on two relationships.. First, the correlation between measured directional permeability (CK, CK_{90}, or CK_h) and core porosity (CPOR), expressed as CK = f (CPOR). Second, the correlation between measured core porosity (CPOR) and the log porosity (NPHI), written functionally as CPOR = f (NPHI). Fig. 17 shows example plots for obtaining these relationships in the Salem and Warsaw Limestone lithozones. In general, the first relationship is poor in all seven wells with very low correlation coefficients between 0.2-0.3. The correlation coefficient varies with lithozones, and is much higher for the Warsaw Limestone (the reservoir) than for Salem Limestone as seen in the Dickman 4 well (Fig. 17a). The second relationship has a higher correlation coefficient of about 0.5 as seen in the Dickman 3a well (Fig. 17b). The above analysis indicates that using permeability estimated from NPHI via CPOR and CK (CK_{90} or CK_h) will introduce uncertainties in the flow simulation. To reduce the risk of losing geological integrity from GR and velocity logs, the two relationships will be further calibrated based on lithozones.

In the Dickman field we have no permeability measurements in the Upper Osage deep saline aquifer, therefore core measurement data were collected from the Upper Osage reservoir of Schaben Field to determine a relationship. The correlation (Fig. 17c, from Fig. 2.6, Carr et. al., 1999) is much better than that seen in Fig. 17a. To obtain the second relationship NPHI logs from the same well with cores will be used with stratigraphic controls on UO1 and UO2 lithozones. Using core permeability from the Schaben Field to estimate the permeability of the deep saline aquifer is feasible because the general control of permeability, as derived from the Upper Osagian core study, is matrix grain size and resulting pore throat size distribution (Carr et. al., 1999). These characteristics can be attributed to the regional depositional environments in which the Upper Osage strata were formed at Schaben and Dickman, roughly similar along the southeast flank of the ancestral central Kansas uplift. However, the estimated permeability may be higher than the actual permeability since the Upper Osage in the Schaben Field is intersecting the Mississippian Unconformity and, therefore, has a better chance to develop conductivity (secondary porosity and permeability) while being exposed.

Using the above two relationships, the permeability values can be estimated from 17 wells for the Salem and Warsaw lithozones, providing enough seed cells to propagating the reservoir porosity and permeability through the 3D model. For the deep saline aquifer with only two data points, the lateral property distribution has to be guided by seismic impedance. For this purpose, impedance logs were computed from two wells and results were cross-plotted with porosity logs (Fig. 18). The relationship has a correlation coefficient around 0.5 to 0.7. However, a good relationship exists mostly in

the Fort Scott lithozones (light-yellow, grey-black and brown, Fig. 18) above the simulation targets rather than in the carbonate reservoir (green, Fig. 18) and saline aquifer (green and blue, Fig. 18). This suggests that obtaining lithozone-based impedance-porosity functions will give a better control in propagation of permeability for the Upper Osage deep saline aquifer.

The above activities in property modeling, focusing on up-scaling property logs for lithozones, provided a good understanding of the 3D distribution pattern of the reservoir porosity in the grid. The semi-quantitative analyses on core and log measurements provided not only methods to derive permeability values from logs and controls on the propagation of properties, but also a measure of risks associated with the flow simulation based on the current input data set.

Geophysics

Activities in geophysics during this reporting period clarified some of the concerns in geological modeling. One major concern is the thin targeted reservoirs (around 20-30 ft) and the deep saline aquifer (170 ft in total), relative to the time window size used to compute seismic attributes. The vertical resolution and detection of seismic data was approximated quantitatively for the Fort Scott Formation. This gives not only a proper thickness range for the lithozone subdivision, but also an estimate on the risk in seismic interpretation and attributes studies. The optimization of the parameter set for seismic attribute computation improved the visualization for features of geological interest.

Vertical Resolution

Vertical resolution of the seismic data is approximately ¼ of the dominant wavelength while vertical detection is approximately 1/25 of the dominant wavelength (Sheriff, 2002). The wavelength is obtained using the relationship: velocity=frequency*wavelength.

To obtain the frequency, seven wells representative of the entire survey area were chosen to ensure that the dominate frequency does not vary laterally with any significance. The frequency spectrum for traces within a 500 ft radius around the sample points and between 0.65 to 0.95 second was extracted using SMT KINGDOM software (Fig. 19). While the overall shape of the spectrum does vary, the dominate frequency is consistently around 45 Hz. Different time window lengths that include the Fort Scott Formation were also evaluated, showing similar results. Fig. 20 is the full frequency spectrum generated around the Elmore 3 well (number 5 in Figure 19) which is approximately in the middle of the survey area and is a good representation of the average frequency spectrum of the entire area. The velocity of the Fort Scott ranges from approximately 13,000 to 18,000 ft/sec with a dominate frequency of 45 Hz. Therefore, taking 15 500 ft/s as the dominant interval velocity we find the wavelength (velocity/frequency) is about 345 ft. The vertical resolution limit is one-quarter of a wavelength or about 86 ft in the vicinity of the Fort Scott. The limit of detectability has various definitions, but using a standard value of 1/16 of a wavelength the limiti of detectability is about 22 ft. The thickness of the fort scott within the Dickman field is between 25 to 30 ft so it is detectable but not resolvable. By the latter is meant that we cannot observe separate top and base reflections. Giving the similar range of average velocity for other lithozones computed (Fig. 14), the thicknesses of these lithozones, except that for the erosional residual of Salem, are above the detectability limit of the data.

The Parameter Set for Curvature Computation

Early in this project (2005-6) seismic volume attributes were computed, but we felt that a careful test of parameters going into the algorithm was needed. Like any processing step, volume attribute results strongly depend on the chosen processing parameters. As a courtesy, Geokinetics, Inc. agreed to reprocess the data for attributes and work with our team to test parameters.

Nineteen attributes have been generated by Geokinetics from the full offset seismic data. Parameters for attribute generation were determined based on acquisition and processing parameters, physical properties of the target area, and resolution limits of the data. Variable parameters, those based on physical properties and resolution limits of the data, were chosen based on test images of curvature. Table 1 lists the parameters used for attribute generation and for all available data sets acquired thus far.
The variable parameters tested in these curvature images are power, lambda, and window length.

While seismic attributes can be dramatic and very useful for interpretation by drawing attention to features not obvious in amplitude data, they do not add any new information beyond what is in the amplitude data they are derived from. Therefore, amplitude data should show hints of features that are more clearly visible in attribute data. Fig. 21 shows an amplitude time slice at 848 ms which approximately corresponds to the top of the Mississippian formation. A channel thought to be an erosional feature due to an unconformity cutting into the Mississippian can be seen in the middle of the survey as well as a fault trending NE-SW in the northern tip of the survey. Values for the variable parameters that best displayed these features were chosen for attribute generation.

Fig. 22 shows four positive curvature time slices at 848 ms. Each image has a different value for the power parameter (0.25 to 3) that relates to a fractional time derivative in the algorithm, all other parameters were held constant as indicated by Table 1. Power values of 1.25 and 3.00 resulted in very noisy, low energy images that would not be useful for interpretation. Values of 0.25 to 0.75 returned data that would be more useful for interpretation, however, 0.25 was chosen for the final power value since known edges of the fault and channel correlated best with curvature features. Similarly, Fig. 23 shows 3 positive curvature time slices at 848 ms with varying values of the lambda parameter (82.5 to 330) that is related to smoothness or average feature size. Again, all other parameters were held constant as indicated by Table 1. A lambda value of 165 returned the image that best illustrated the two key features.

These tests were conducted using a window length of 10 ms which would average over a thickness of 100 ft using an average velocity of 10,000ft/s. While most formation thicknesses are well below 100 ft, these attributes seem to be insensitive to this parameter as shown in the two test images in Fig. 24 (window lengths of 10 and 6 ms, respectively). Apart from consideration of formation thickness, the window parameter is related to local slope estimates that drive the volume attribute calculations. The results were not very sensitive to this parameter, but 10 ms seemed slightly better.

The curvature time slices computed using the optimized parameter set were used to compare with the ANT results to identify the NE-oriented faults/fractures and the buried features relating to karst topography as described in the Geology section.

Reservoir Simulation

After thorough research on reservoir simulators used in CO2 sequestration simulation (Dec. 31, 2008 report), the CMG simulator by Computer Modeling Group Ltd. was chosen because of its clearly leading position in research and field application for CO2 sequestration simulation. During this report period, we successfully persuaded the Computer Modeling Group Ltd. to donate the CMG simulator to the University of Houston. Using the CMG Grid Builder tool, a preliminary 3D flow simulation grid was established with input top maps and thickness isopach from the Petrel model, for the LC Sandstone and the Upper Mississippian reservoirs. An in-depth pre-simulation data assessment was completed to serve as input for a "history match" process.

We are planning to compare simulation results using CMG and ECLIPSE, but the grid building and testing will be done in CMG. Final run comparisons with ECLIPSE will then be done.

Dickman Flow Simulation Grid

The preliminary Dickman field simulation grid has been completed by using CMG Grid Builder (Fig. 25). The grid consists of two geological layers with tops and thickness isopach exported from the Petrel M2 model: the Lower Cherokee Sand clastic reservoir and the Upper Mississippian carbonate reservoir. The grid cell is 50 by 50 ft in the X-Y plane with 2500 cells in total, covering an area of about 3 by 3 miles.

For the preliminary experiment runs, the two reservoir layers will be divided into several layers during the flow simulation. The results from the two reservoir layers that are different in lithology will be compared. A more detailed geological grid from Petrel M3 model will be loaded for further experiment runs.

Dickman Field Data Assessment

A pre-simulation data assessment serves as the base for a history match process before the predictive simulation. History match aims at matching past oil production data by calibrating or modifying reservoir properties obtained from geological modeling and other sources. A data set including production, DST, and data from geological modeling was compiled during this report period.

Dickman Field was discovered and put into production in 1962 (Hilpman et al., 1964). The general information of the Upper Mississippian reservoir in the survey area is:

Acreage = 240 acres
Net pay zone thickness = 7 feet
Average depth = 4424 feet in MD
Oil API gravity = 37 API
Original oil in place = 2 ma bbl (calculated at porosity=20% water saturation=20%) as computed by the following:
7758 (bbl per acre-foot) * 7 * 240 * 0.2 * (1-0.2) = 2 million bbl.

The production data at the end of 2008 are as follows: (data from Grand Mesa Company)

Total number of production wells = 20, no gas production

Cumulative oil production = 2,053, 000 bbl

Drive = bottom water drive

Water cuts = around 98% for current producing wells, indicating a very high recovery rate

The drill stem tests from two wells at Mississippian pay zones gave further information on reservoir properties:

Temperature at the bottom of the hole = 121^{o} F

Reservoir Temperature (computed from the pressure gradient) = 110^{o} F

Average Pressure = 2200 psi

The above data set, together with the reservoir properties obtained from geological modeling and other sources, has been imported into the Simulator for history matching.

Work Plan for Next Quarter

Geology

Geology work in plan will focus on maximizing the geological integrity in quantifying deterministic Petrel models and minimizing the information loss in simplifying the simulation grid for computing efficiency. Four major tasks are planned to resolve important issues observed in the Petrel M3 model, one for the Structural Modeling and one for Fault Modeling phases (deterministic modeling), and two for the Property Modeling phase (statistical and conceptual modeling).

The first task is to correct misties of the time-depth conversion in M3 Model. A careful QC on M3 Model revealed a significant increase of pay zone volumes above the OWC due to misties in the time-depth transfer around the Dickman Field. Unlike the south part of the survey where four wells penetrating the entire deep saline aquifer, there is no well penetration in the north area of the survey where the Dickman Field is located. The lack of velocity control for the deep saline aquifer there may be improved by adding a pseudo-TDR using zone-average velocity computed for the deep saline aquifer in the south part of the survey (Fig.14). The corrections are expected to give a total reservoir volume with acceptable precision after the time-depth conversion. The seismic impedance volume will then be converted to depth domain with zone-specified impedance values which will be normalized to have the similar unit of porosity. The resulting impedance values will serve as a secondary control for porosity propagation in the deep saline aquifer.

The second task is to correct the zone-averaged neutron porosity (NPHI-limestone) based on lithology. Our version of "Petrel Property Modeling" does not have the bulk scaling functions. Therefore, manual correction by the overlay of lithology curves on cross plots will be conducted lithozone by lithozone. The three scaling curves for sandstone, limestone, and dolomite porosity were already input into Petrel for this purpose. After the porosity is correctly scaled for dolomite contents, the permeability will be computed from the resulting porosity using the two relationships as discussed in the previous section for Property Modeling.

The third task is to refine the fault model combining the ANT and curvature analysis results and the geological understanding. Emphasis will be on identifying the NW-trending faults and fractures that were not well-resolved by the previous study. Because they were considered as flow conduits, their existence could become an important factor to control both reservoir conductivity and seal leakage prediction in flow simulation.

The fourth task is to resolve the mismatch of zone-averaged properties between wells with partial penetration to lithozones, revealed by zone property maps and property cross-plots with zone filters. For instance, zone-average porosity computed in a partially penetrated Salem Limestone lithozone in one well was mismatched to the partially penetrated Warsaw Limestone lithozone in another well. It is likely a software bug in handling partially penetrated lithozones and the lack of zone versioning options. Unless enhancements are provided by the donor company, an easy solution is to keep two versions of the Petrel model running together to address two aspects of the modeling process. In one version of the model, all missing tops due to partial or no penetration will

be manually assigned the same MD as the last penetrated top in each well. This will give a correct match of zone-averaged properties between wells in Property Modeling and data analysis. Such a model can compute porosity and permeability based on lithozones to assign to seed cells. However, it will give only penetrated thickness rather than the geological thicknesses of lithozones in a stratigraphic framework. The second version of the model will be used to retain the geological thickness of lithozones, considering full, partial or no penetration, by combining well top and seismic data. The second model will take cell assignments with values from the first model, to serve as a framework for the CMG flow simulator.

Geophysics

Two major tasks are planned to improve the time-depth conversion of the simulation model. First, improve the precision of well and seismic correlation of the Fort Scott Formation Top. Second, Extend the time-depth tie to the Stone Coral Formation above the Fort Scott datum.

The first task is to re-build the synthetic. Four synthetic seismograms were in GeoFrame before 2008 and gave rise to the seismic stratigraphic framework for report periods before Mar. 31, 2008 report. The seismograms on GeoFrame were not transferable to Petrel, and the stratigraphic framework was revised based on time-depth pairs (shown Dec. 31, 2008 report). Therefore it is necessary to complete the synthetic study, to correct and support the seismic stratigraphic framework used in the Petrel modeling work.

The second task is to establish a regional velocity model for the survey area. The velocity model used to convert the simulation in Petrel is based on data obtained at or below Fort Scott top (the hanging datum). The lack of interval velocity above the Fort Scott Top may be one of the causes of these misties. Stone Coral Formation is about 2600 ft above the Fort Scott Formation top (near the sea-level) and is well identified in well logs. Obtaining a precise well-top and seismic tie at the Stone Coral Formation, the interval velocity for strata above the Fort Scott hanging datum will help to improve the precision of time-depth conversion for the model.

Reservoir Simulation

The flow simulation work will focus on the following two tasks: 1. complete an in depth simulation data assessment; 2. run history matching to optimize the Dickman simulation grid model.

A simple grid containing only two layers as shown in Fig. 25 is suitable for the initial data assessment. The speed of computing is affected by the number of layers included in the model. It takes a laptop one minute to 10 minutes to complete a forty-year history matching run with this simple grid. The completion of the simulation data assessment will provide confidences on the input data to conduct the simulation convergent study. A series of more complicated grids will then be used for runs until an optimal simulation grid by which the difference in solutions from two consequent runs is below the threshold.

Cost Status

Baseline Costs Compared to Actual Incurred Costs

2009 Jan 1 – Mar 31	Plan	Costs	Difference (Plan-Costs)
Federal	$33,333.	$36,098	($2,765)
Non-Federal	$12,563.	$0	$12,563
Total	$45,896.	$36,098	$9,798

Forecasted cash needs vs. actual incurred costs

Notes:

1. Federal plan amount based on original award of $400K averaged over 12 reporting quarters.
2. Cost this period reflects 3 months salary for J. Zeng and H. King, and 2 months for P. Geng
3. Non-Federal plan amount based on original budget cost share of $150,573 averaged as above.

Analysis of Variance

Actual Progress Compared to Milestones

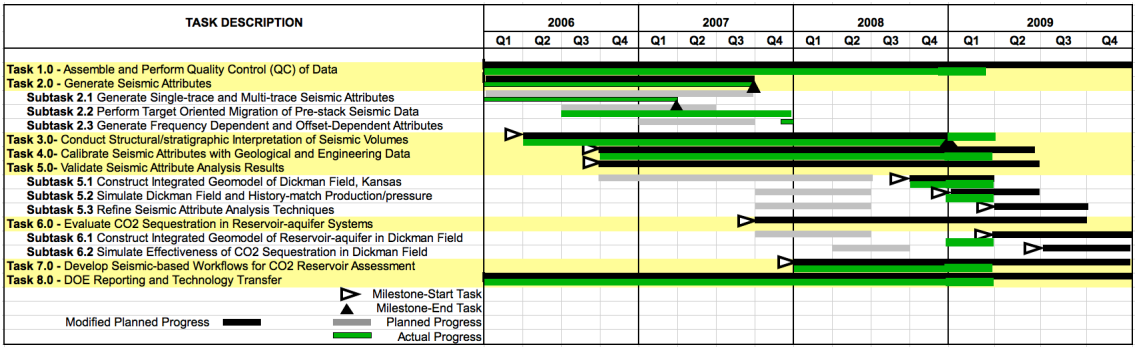

Summary of Significant Accomplishments

Problems and Significant Events

We are happy to report no problems in this reporting period.

Continuing Personnel

Prof. Christopher Liner is Principle Investigator and lead geophysicist. He is a member of the SEG CO2 Committee and Director of the U Houston Reservoir Quantification Lab.

Dr. Jianjun (June) Zeng has been working exclusively on this project since Dec 2007 and is lead geologist. She will be funded through the end of 2009.

Heather King is a graduate MS student in geophysics who joined the project in January 2009 as a research assistant. She will be funded out of the project Jan-May and Sept-Dec 2009, when she anticipates graduating. Her thesis will focus on Fort Scott to demonstrate the integrity of this formation as a seal for injected CO2. This will involve subtle structure and stratigraphy inferred by interpretation of multiple seismic attributes.

Dr. Po Geng has been working on this project as a specialist consultant since February, 2009. He will be funded out of the project, considered part-time, through the end of 2009.

Technology Transfer Activities

An abstract on the Dickman CO2 sequestration simulation was submitted to the SEG, 2009.

Contributors

University of Houston
Christopher Liner (P.I, Geophysics)
Jianjun (June) Zeng (Geology and Petrel Modeling, primary author of this report)
Po Geng (Flow Simulation)
Heather King (Geology and Geophysics)

References

Blakely, R., 2004, Paleogeography and Geologic Evolution of North America, URL: http://jan.ucc.nau.edu/%7Ercb7/nam.html

Carr, T. R., D. W. Green, and G. P. Willhite, 1999, Improved oil recovery in Mississippian carbonate reservoirs of Kansas: Near term-class 2, Annual Report Submitted to US Department of Energy (DOE), Report no. DOE/BC/14987-10, 168.

Cole, V. B., 1976, Configuration of the top of the Precambrian rocks in Kansas: Kansas Geological Survey, Oil and Gas Investigations 26--Map M-7, scale 1:500000

Gerhard, L. C., 2004, A new look at an old petroleum province: Kansas Geological Survey, Current Research in Earth Sciences, 250, part 1.

Franseen, E. K., T. R. Carr, W. J. Guy, and D. S Beaty, 1998, Significance of depositional and early diagenetic controls on architecture of a Karstic-Overprinted Mississippian (Osagian) reservoir, Schaben Field, Ness County, Kansas: Presented at the AAPG Annual Meeting.

Franseen, E. K., A. P. Byrnes, J. R. Cansler, D. M. Steinhauff, and T. R. Carr, 2004, The Geology of Kansas—Arbuckle Group: Kansas Geological Survey Bulletin, Current Research in Earth Science, 250, part 2.

Franseen E. K., 2006, Mississippian (Osagean) Shallow-water, mid-latitude siliceous sponge spicule and heterozoan carbonate facies: An example from Kansas with implications for regional controls and distribution of potential reservoir facies: Kansas Geological Survey, Current Research in Earth Sciences, 252, part 1.

Gerhard, L. C., 2004, A new look at an old petroleum province: Kansas Geological Survey, Current Research in Earth Sciences, 250, part 1.

Hilpman P. L., M.O. Oros, D. L. Beene and E. D. Goebel, 1964, Oil and Gas Development in Kansas during 1963: State Geological Survey of Kansas Bulletin, 172.

Kansas Geological Survey (2009), Kansas Well Top Stratigraphic Viewer, State Geographic Information System, KGS.

Kansas Geological Survey (2009), Brine Analyses in Kansas: Oil and Gas Production Data, KGS.

Merriam, D. F., 1963, The Geologic History of Kansas: Kansas Geological Survey Bulletin, 162.

Moore, R.C., 1949, Divisions of the Pennsylvanian System in Kansas: Kansas Geological Survey Bulletin, 83.

Newell, K. D., W. L. Watney, D. W. Steeples, R. W. Knapp, and S. W. L. Cheng, 1989, Suitability of high-resolution seismic method to identifying petroleum reservoirs in Kansas-A geological perspective, *in* D. W. Steeples ed., Geophysics in Kansas: Kansas Geological Survey Bulletin, 226, 9-30.

Nissen, S. E.,T. R. Carr, and K. J. Marfurt, 2006, Using New 3-D Seismic attributes to identify subtle fracture trends in Mid-Continent Mississippian carbonate reservoirs: Dickman Field, Kansas, Search and Discovery, Article #40189.

Nissen, S. E., K. J. Marfurt, and T. R. Carr, 2004, Identifying Subtle Fracture Trends in the Mississippian Saline Aquifer Unit Using New 3-D Seismic Attributes: Kansas Geological Survey, Open-file Report 2004-56.

OuYang. J., 1994, Well Log Interpretations and Reservoir Descriptions: Book Series on Petroleum Exploration in the Tarim Basin, 9, 235–291.

Sheriff, R. E., 2002, Encyclopedic Dictionary of Applied Geophysics, Fourth Edition: Society of Exploration Geophysics.

Zeller, D. E., 1968, The Stratigraphic Succession in Kansas, 1968: Kansas Geological Survey Bulletin, 189.

Tables

Data type	Creator	Parameter		Value	Units
Pre stack time migrated stacks	Kurt Marfurt	area		3.325	mi^2
		inlines		158	
		crosslines		169	
		spacing		82.5	ft
		offset angle	all	0-45	degrees
			near	0-10	
			mid	10-20	
			far	20-30	
Acoustic Impedance Volume	Jenny Zhou using STRATA (Hampson-Russell program)	stack		all	angle
Elastic Impedance Volume				near and far	angle
Geometric attributes	Geokinetics Peg Guthrie	lambda		165	
		power		0.25	
		window length		10	ms
		time window		0-1.6	s
		max dip angle		20	degrees
		average velocity		10,000	ft/s
		power		0.25	

Table 1. Parameter set used in used for attribute generation and for all available data sets acquired

Figures

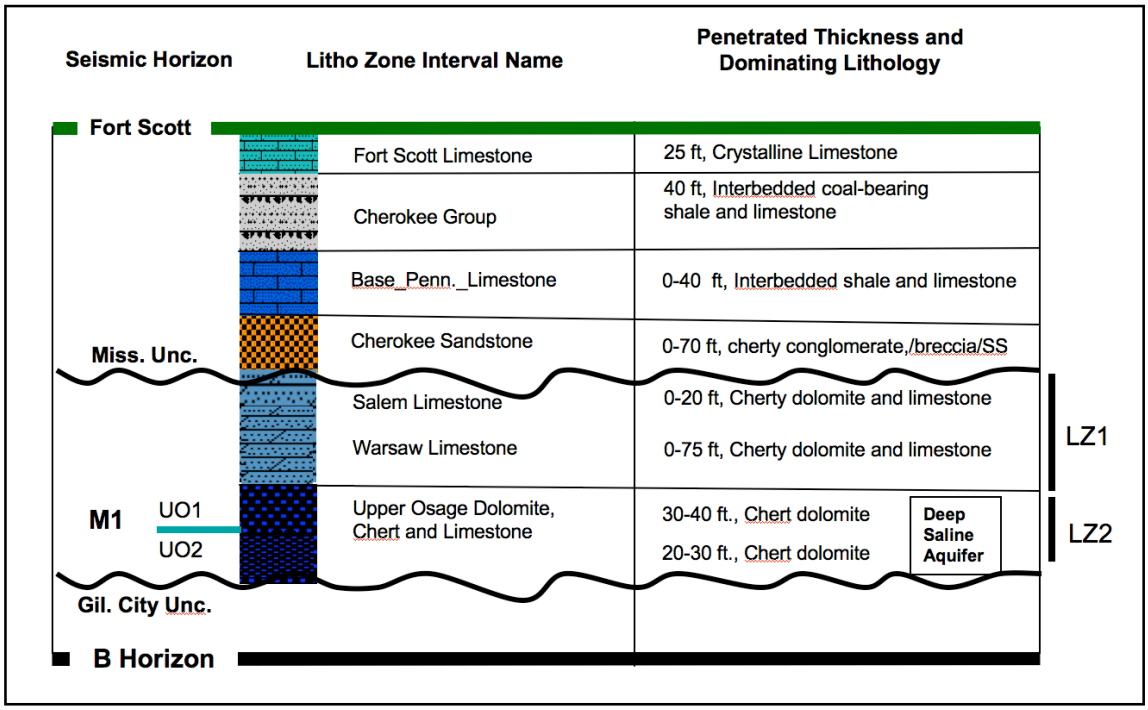

Fig. 1. Up-dated stratigraphic column showing Fort Scott Horizon (green) as the hanging datum of the structure model, the B Horizon (black) as the base of the structure model, and new lithozones (LZ1, LZ2) beneath the Mississippi Unconformity (blue) for the property modeling: Salem Limestone (shaded in light blue with course layering pattern), Warsaw Limestone (shaded in light blue with finer layering pattern), the M1 Surface (light blue) separating the Upper Osage lithozone 1 (UO1, dark blue above M1) and Upper Osage lithozone 2 (OU2, dark blue above M1), and the Gilmore City Horizon (GCU), an unconformity below the Upper Osagian. The Upper Osage in the survey area makes up the deep Saline aquifer.

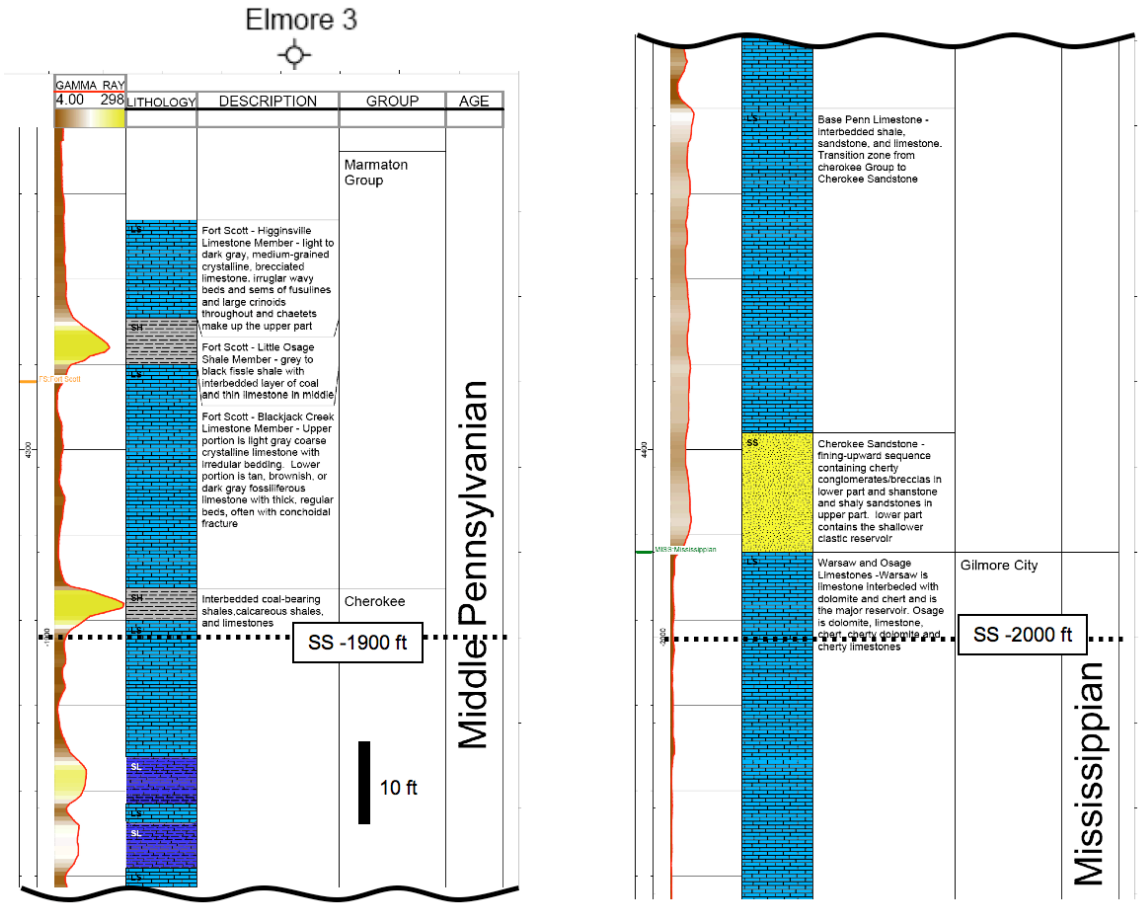

Fig. 2. Composite Log for Well Elmore 3 consisting of seven tracks: age, depth (ft), gamma ray (API), lithology (interpreted from the gamma ray log), description, group, and formation. Formation lithology was generalized into four categories: shale, limestone, calcarious shale, and sandstone. While there are many more lithologies present within these formations, the non-uniqueness of the gamma ray log interpretations makes many units difficult or impossible to differentiate to any greater detail. The Fort Scott Formation has been divided into member groups while all others have been interpreted at a larger scale, with exception of several easily identifiable units.

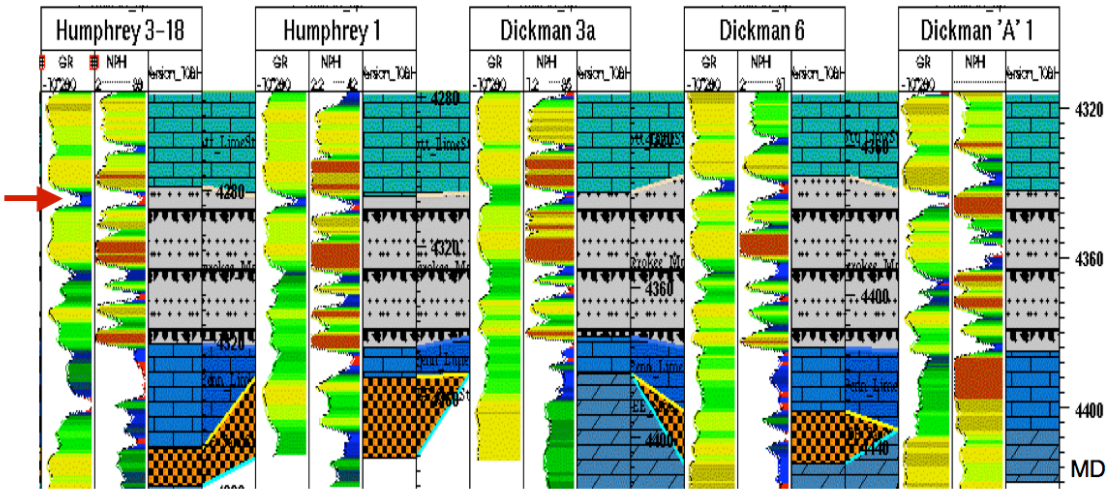

Fig. 3. A well cross section showing the thickness variation of the Fort Scott Limestone for the survey area from west to east. The cross section is hung on the top of the Fort Scott Limestone (in light blue). A shale layer with remarkable High GR (red arrow) below separates the Froe Scott Limestone from the underlying Cherokee Group (in grey). The thickness of the Fort Scott Limestone is almost uniform through the entire survey area, about 25-30 ft.

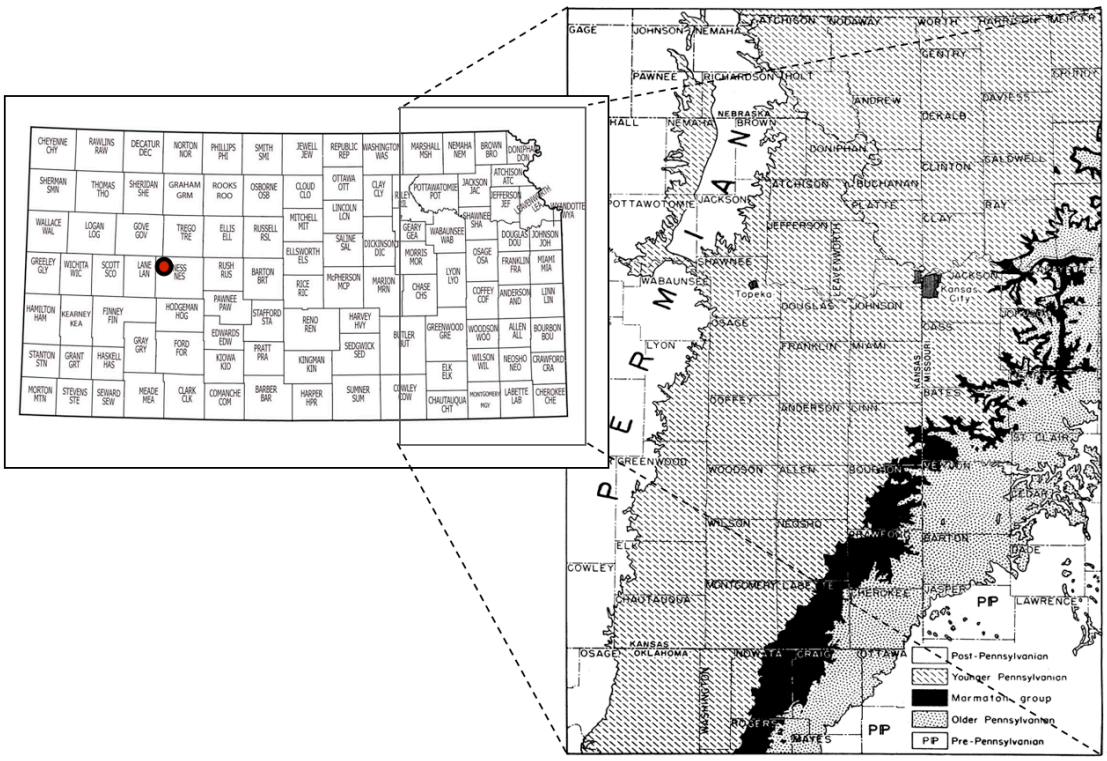

Fig. 4. Distribution of Marmaton outcrops (black) in Kansas and parts of adjoining states. The Marmaton group comprises the upper part of the Desmoinesian Series of Pennsylvanian rocks in the northern midcontinent region (Moore, 1949). The Fort Scott Limestone is the lowest formation in the Marmaton Group. Kansas state map insert shows location of mapped area (dashed) and the Dickman Field (circle)

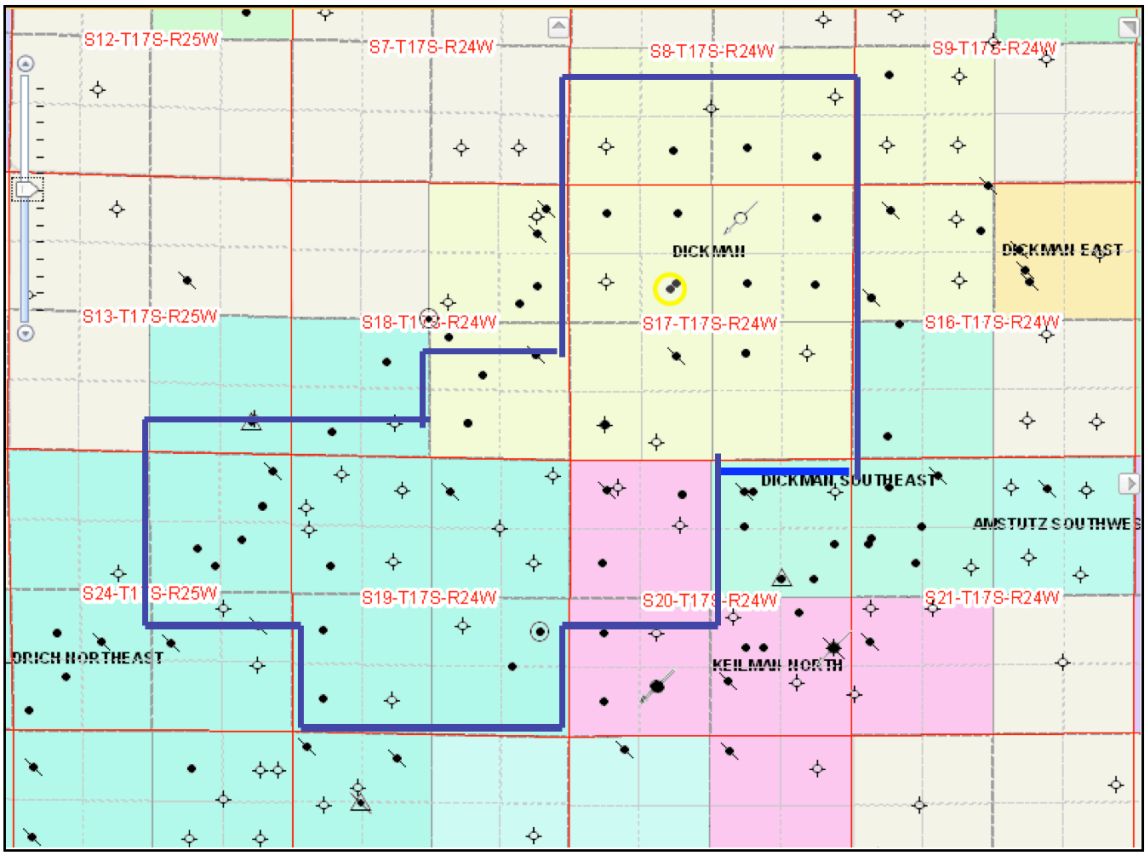

Fig. 5. The map of the oil fields included in the merged survey area. The merged survey area covers most of the Dickman Field, the north parts of the Aldridge Northeast and the Keilman North Fields, and north margin of the Dickman Southeast Field

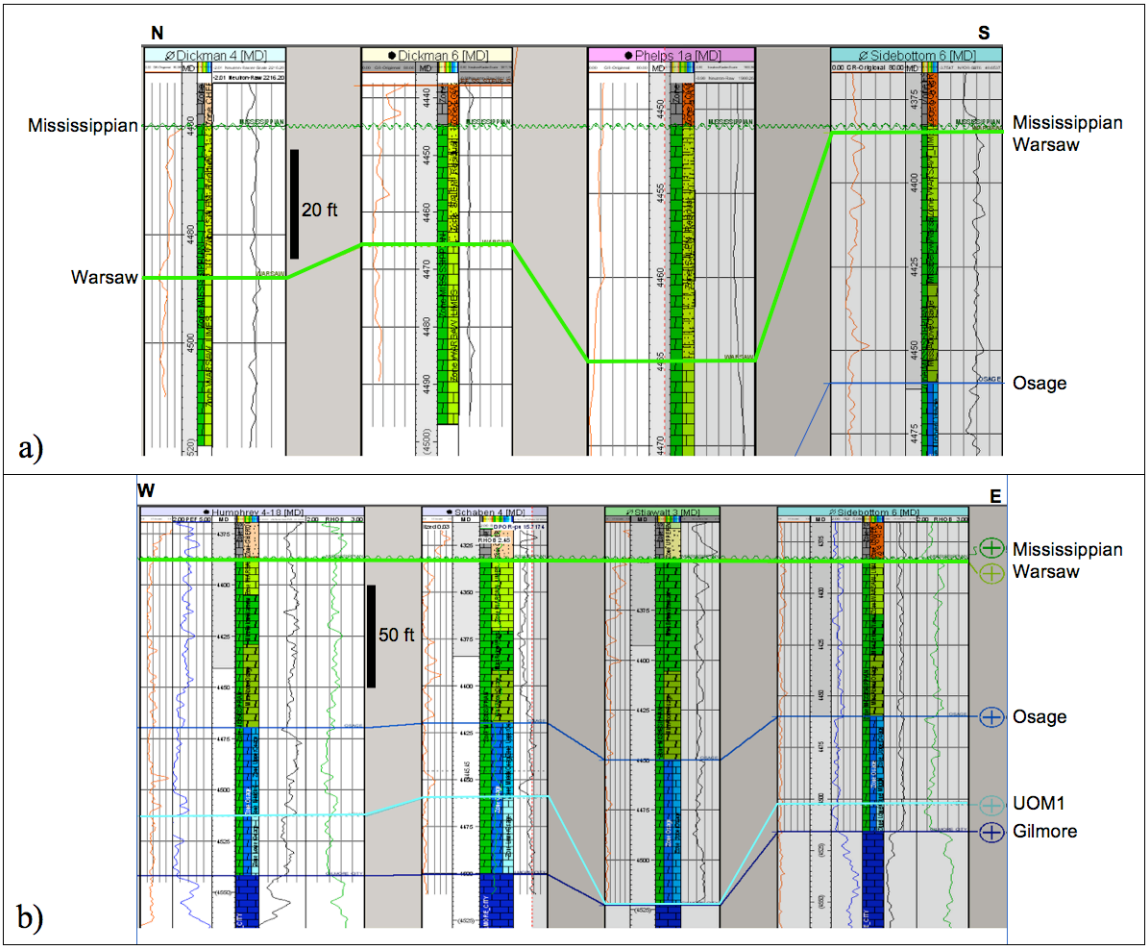

Fig. 6. Well cross section showing the subdivisions of Upper and Lower Mississipian strata. Sections are hung on the Mississippi unconformity (light green wavy line). Logs to the right of the lithology column are porosity (black) and density (blue); and to the left of the lithology column are normalized GR (Brown) and PE (blue). The oil water contact is shown as a dot line in purple. a). Cross section through a few wells in which the Upper Mississippi Salem Limestone and Warsaw Limestone are differentiated by the Warsaw top (light green). Salem Limestone is around 20-30 ft to the north, and is only 2 ft to the south in SideBottom 6. The Dickman 4 well produces from Salem, and the Phelps1a is a production well from Lower Cherokee Sand. Well Dickman 6 is an injector and Sidebottom 6 is a saltwater disposal well to deep saline aquifer. The Salem/Warsaw contact is not clear in Dickman 6. b). Cross section through four wells with full penetration of Mississippian carbonate reservoir and deep saline aquifer. The entire section is in the south part of the survey. The lithology column contains lithozones in Upper (green) and Lower Mississippian (light blue). The Salem is not identified in most wells except in Sidebottom 6 to the east. The section also shows the UO1 and UO2 lithozones above and below the OUM1, respectively. The dark blue zone beneath the Gilmore City unconformity is beyond the target of this project. The Humphrey 4-18 to the west is producing from Mississippian reservoir. The Schaben 4 next to it is producing from a shallower reservoir in the Cherokee Group above the target of this study. The Stiawalt 3 is a salt water disposal well into the deep saline aquifer, similar to the SideBottom 6.

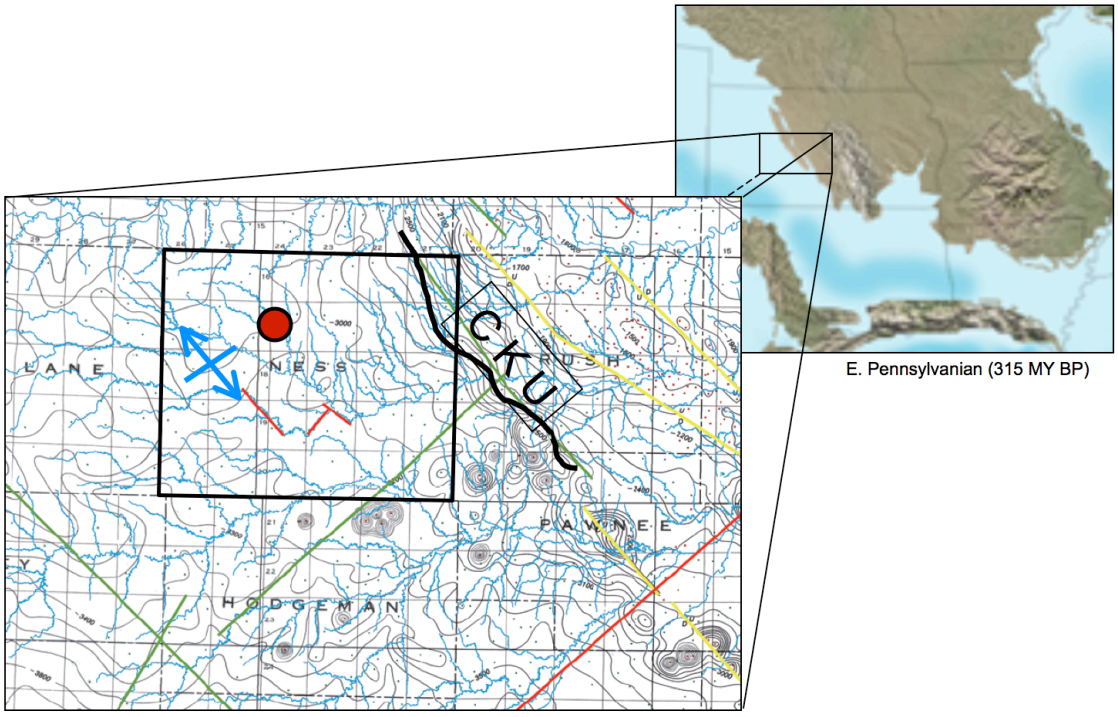

Fig. 7. Pre- and Post Mississippian structure framework in Ness County. The map to the upper right is the regional paleo-geography approximately 315 million years BP (early Pennsylvanian time) showing the structural location of the survey area (Blakely, 2004). The main map (Gerhard, 2004) to the lower left is contoured on depth to basement and outlines lineament trends, reflecting interpreted basement structural elements. The location of the Dickman Field area is shown by red circle. The boundary of Post-Mississippian Central Kansas Uplift (CKU) is in black. The dark blue lines show a secondary anticline with the axis perpendicular to the CKU. The yellow, red and green lines represent linears interpreted from Cole (1976), from drainage anomalies, and from potential field information.

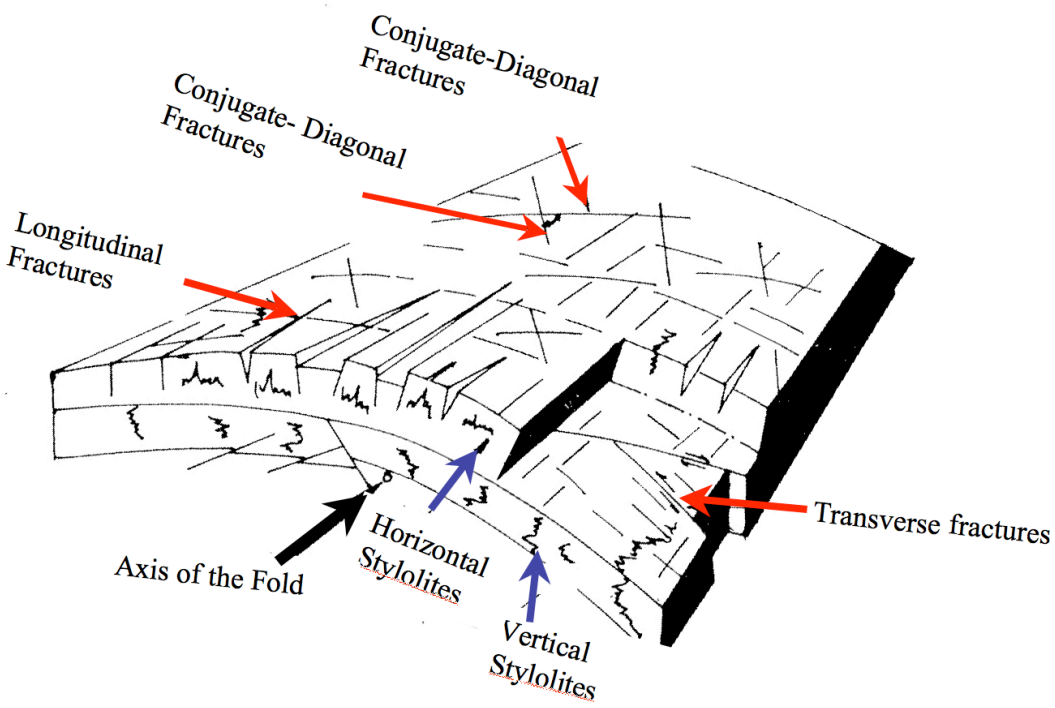

Fig. 8. Ideal types of linear features related to the structural deformation of carbonates from a 3D simulation model (figure from Fig. 5-7, OuYang, 1994). Red arrows indicate brittle fractures related to the regional stress filed, most vertical to the strata tops, and blue arrows indicate stylolites by pressure-solution, vertical or almost parallel to the strata tops.

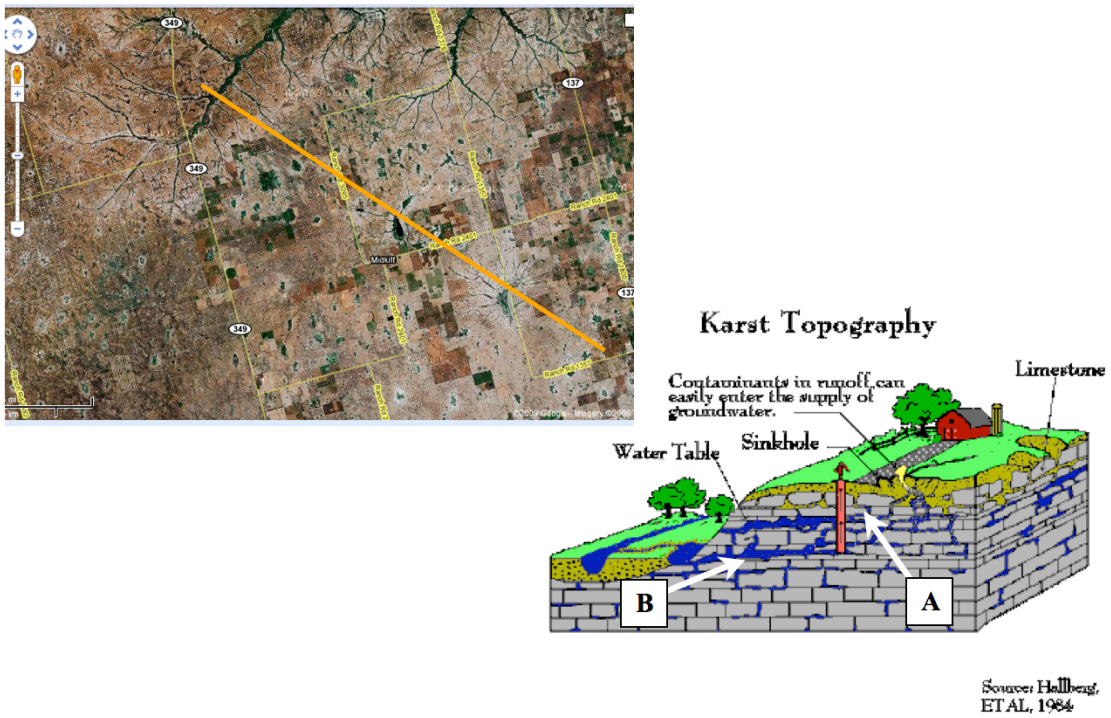

Fig. 9. Karst systems develop by carbonate dissolution along plans of weakness. The map to the upper left shows resent day karst features (Google Earth, western Texas). The block diagram to the lower right shows vertical profile along an imaginative section (brown line) showing the 3D distribution of the karst features. In map view, the preferred orientations as indicated by sinkholes and the drainage pattern are mostly related to fracturing in the strata (along red lines). In 3D subsurface view, sinkholes develop mostly at intersections of vertical fractures (A) as do surface valleys during early Karst development. Horizontal Karst features, such as underground tunnels, developed near the water table afterward (B), may enlarge, fill with breccias, and finally collapse to become surface channels during the late Karst development.

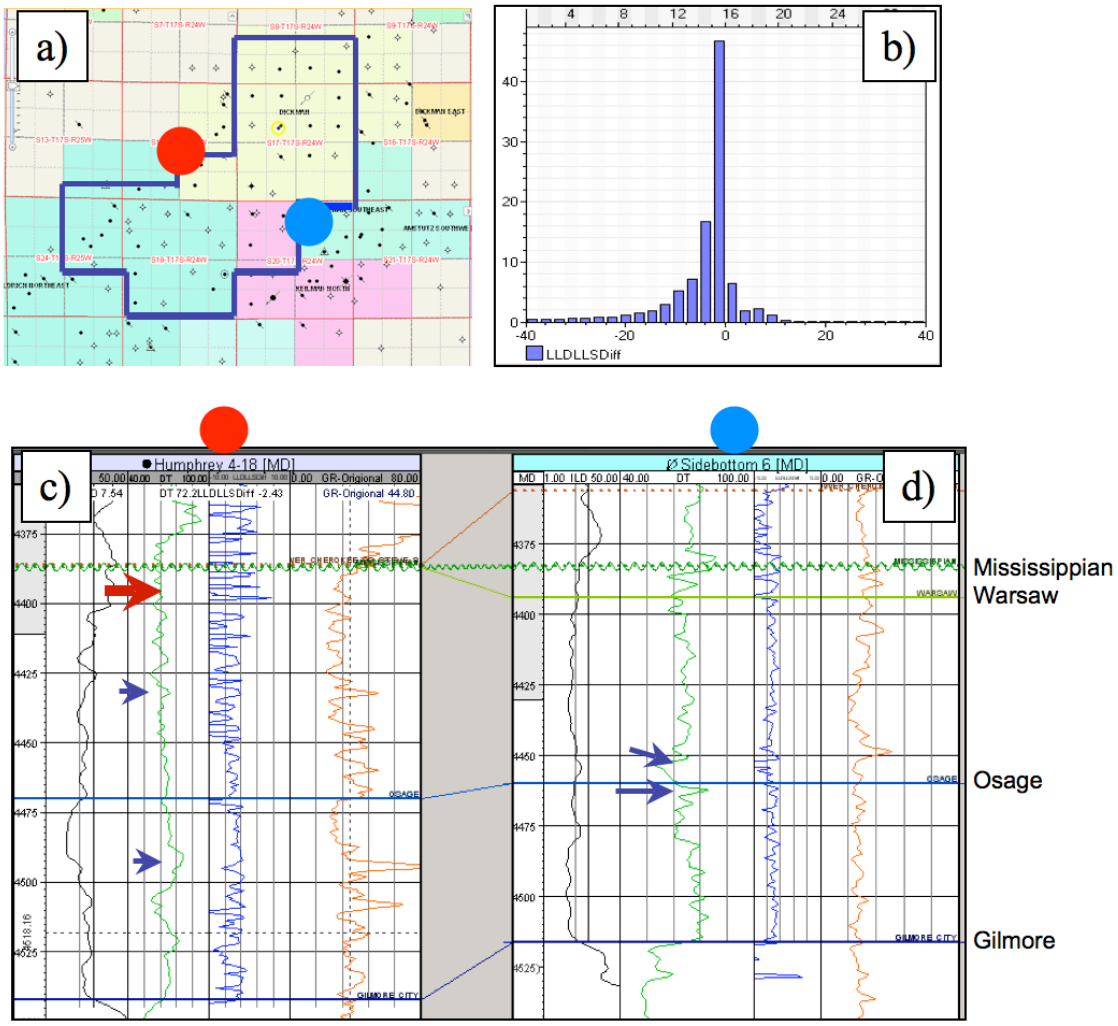

Figure 10. Log indicators for fractured zones for two wells with GR, DT, RLD and RLS logs at the boundary of the survey area. (a) Map showing log locations. (b) Histogram of deep minus shallow electrical induction. (c) Humphrey 4-18 well, and (d) Sidebottom 6 well. The logs in each well panel, from right to left, are: GR in brown, (RLD-RLS) in blue, DT in green, and ILD in black. The Mississippi Unconformity is shown as a green wavy line. The pay zone below Miss. unconformity (red arrow) in Humphrey 4-18 has very high RLD values (oil in formation) and many positive RLD-RLS peaks kicking to right and negative peaks kicking to left. Possible fractured zones (blue arrows) are with lower ILD, decreasing RLD-RLS, and GR and/or DT peaks. The histogram shows the distribution of RLD-RLS values for all Mississippian carbonate lithozones. Over 80% of the readings (the peak) are negative from -10 to 0. Less than 10% of readings are positive, from 0 to +10, indicative of fractured zones or pay zones (when interpreted with other log indicators)

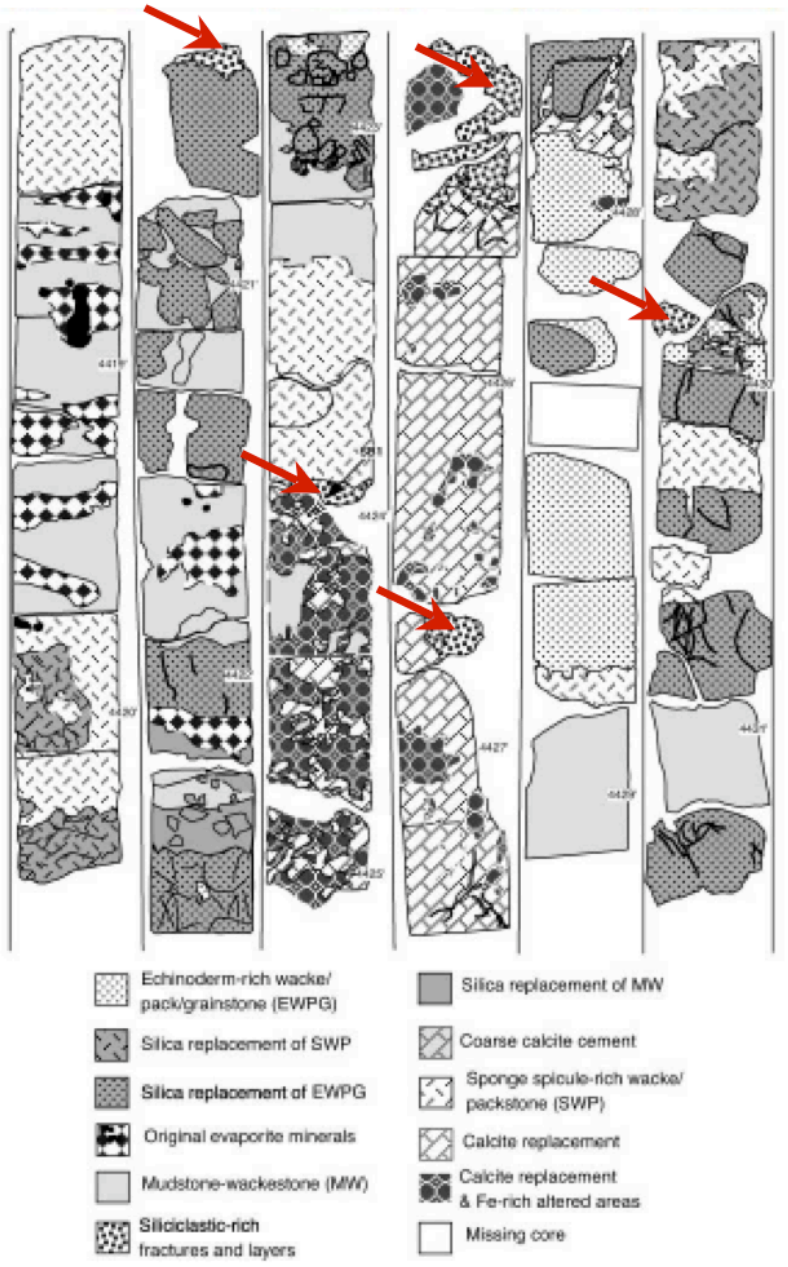

Fig. 11. Schaben Field core description of Upper Osage, showing fractures of structural and non-structural origins. The red arrows indicate the siliciclastic-filled fractures and layers that might associated with the Post-Mississippi up-lift. However, whether they reflect structural fractures penetrating the entire strata is beyond the scope of cores. (Picture is from Franseen, 1998, original resolution is low)

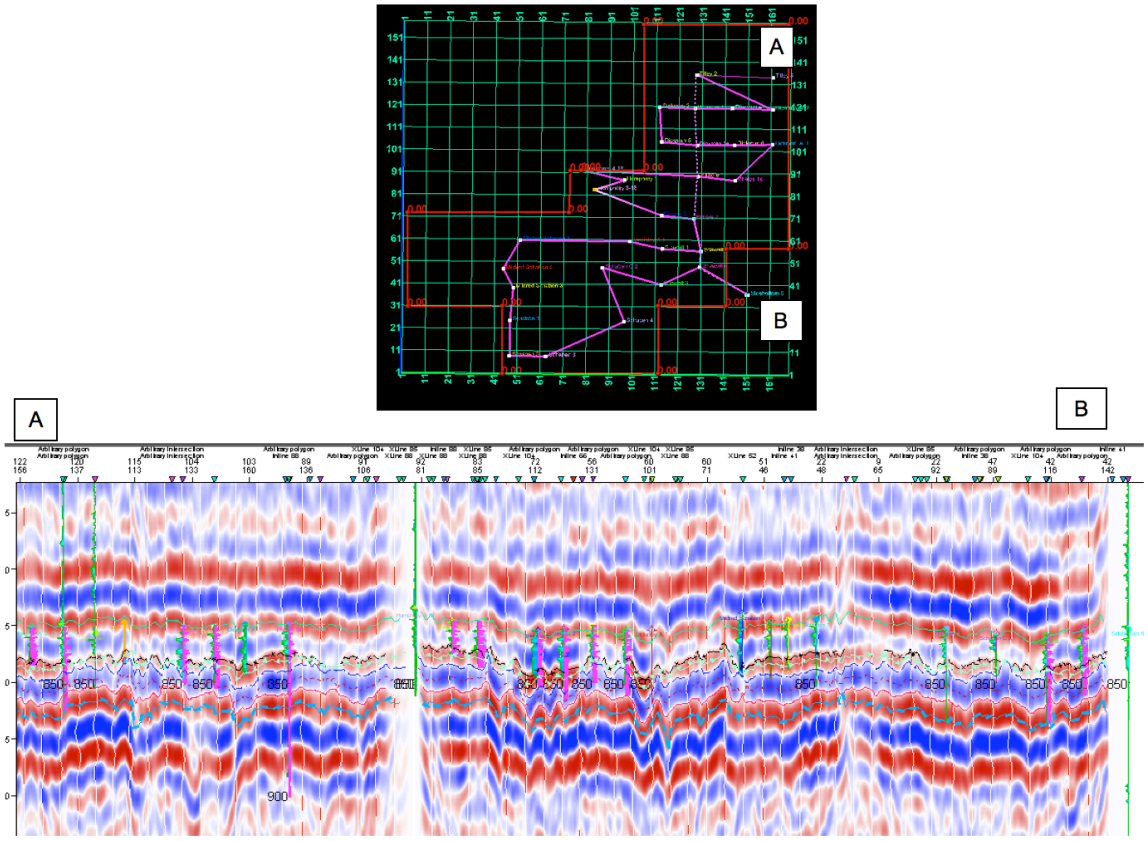

Fig. 12. Log-seismic overlay for the correlation of lithozones. Upper: map view of a cross section connecting all wells with logs or core data, lower: seismic-well log tie for the above section. The interpretations of the new horizons separating lithozones were checked on these wells as close as possible. The interpreted horizons were then converted to the surfaces in the 3D grid.

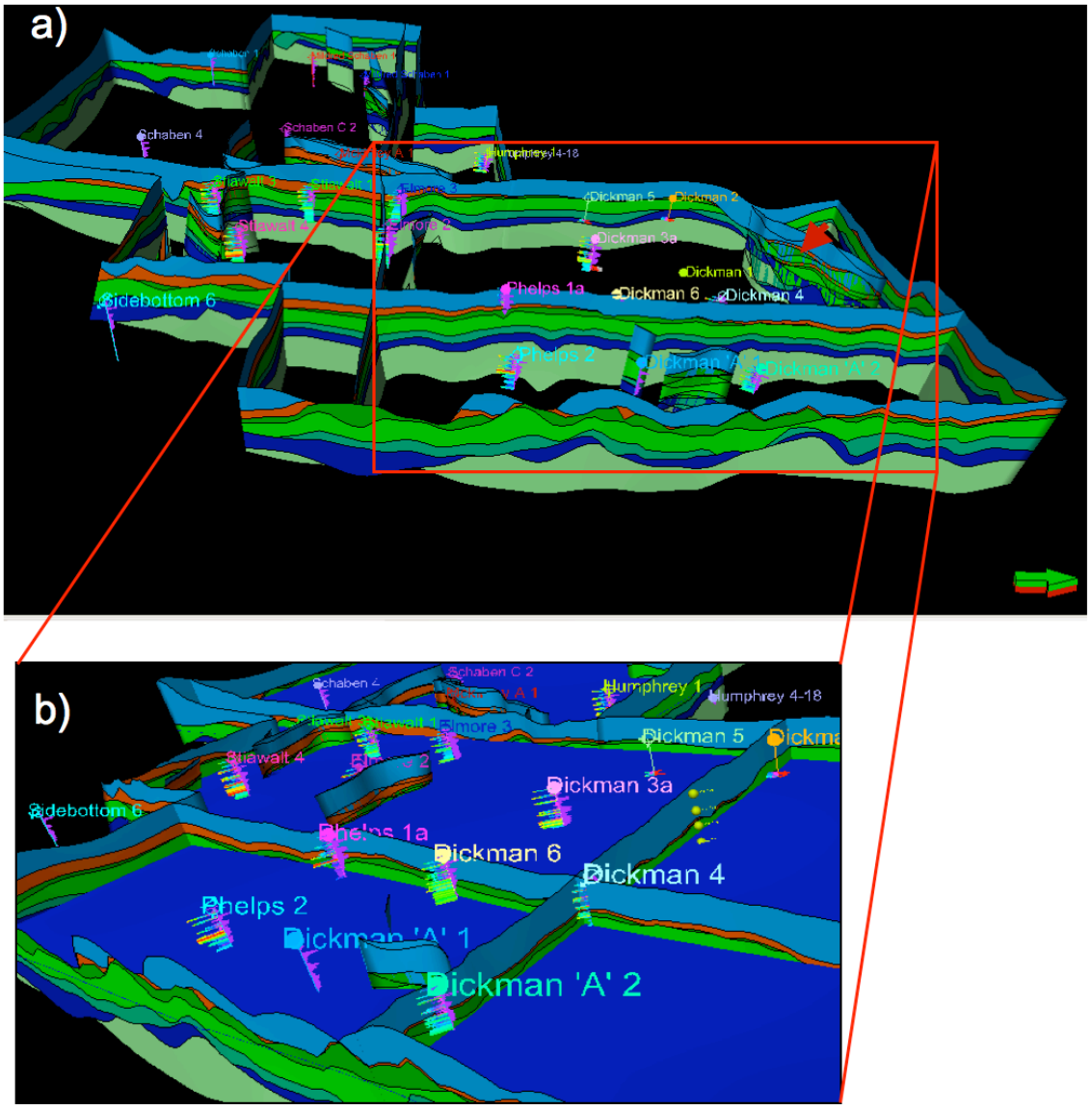

Fig. 13. 3D grid with newly added lithozones, Z is in TWT. Vertical exaggeration is 20:1. The top and the base of the grid are removed to show the interior of the stratigraphic and structural framework. a) The structure model viewed from east of the survey area. Lithozones are shown by color bends at model edges and intersections. From top to bottom they are: Fort Scott (light blue) as seal, Cherokee sandstone containing the Lower Cherokee sandstone reservoirs (brown), Mississippi Unconformity, the Upper Mississippi Salem (green) and Warsaw (light green) containing the carbonate reservoirs (partially saline aquifers), and the Lower Mississippi Upper Osage OU1 (bluish-green) and OU2 (greenish-blue) lithozones consisting the deep saline aquifer. The dark blue below Gilmore City is below the target of this project. The bottom of the very light green zones is the base of the structure model, uncut by fault planes as required by the modeling process. Color and style for well logs: GR pink to right, Neutron porosity blue to left. Logs at the purple arrows are the core porosity (pink to right) and permeability (blue to left). Major fault planes are included, such as a fault to the north corner of the survey that caused displacement of the strata. b) A part of the model viewed from the northeast around the Dickman Field. Blue surface is the oil/water contact, above it lays the Salem/Warsaw reservoir around the Dickman Field area. The Dickman 2 Dickman 4 and Dickman 5 have core porosity and permeability measurements from the producing zone. In Dickman 1a production is partially from Lower Cherokee Sand and at Phelps1a to the south (right), the pay zone is mostly from this interval.

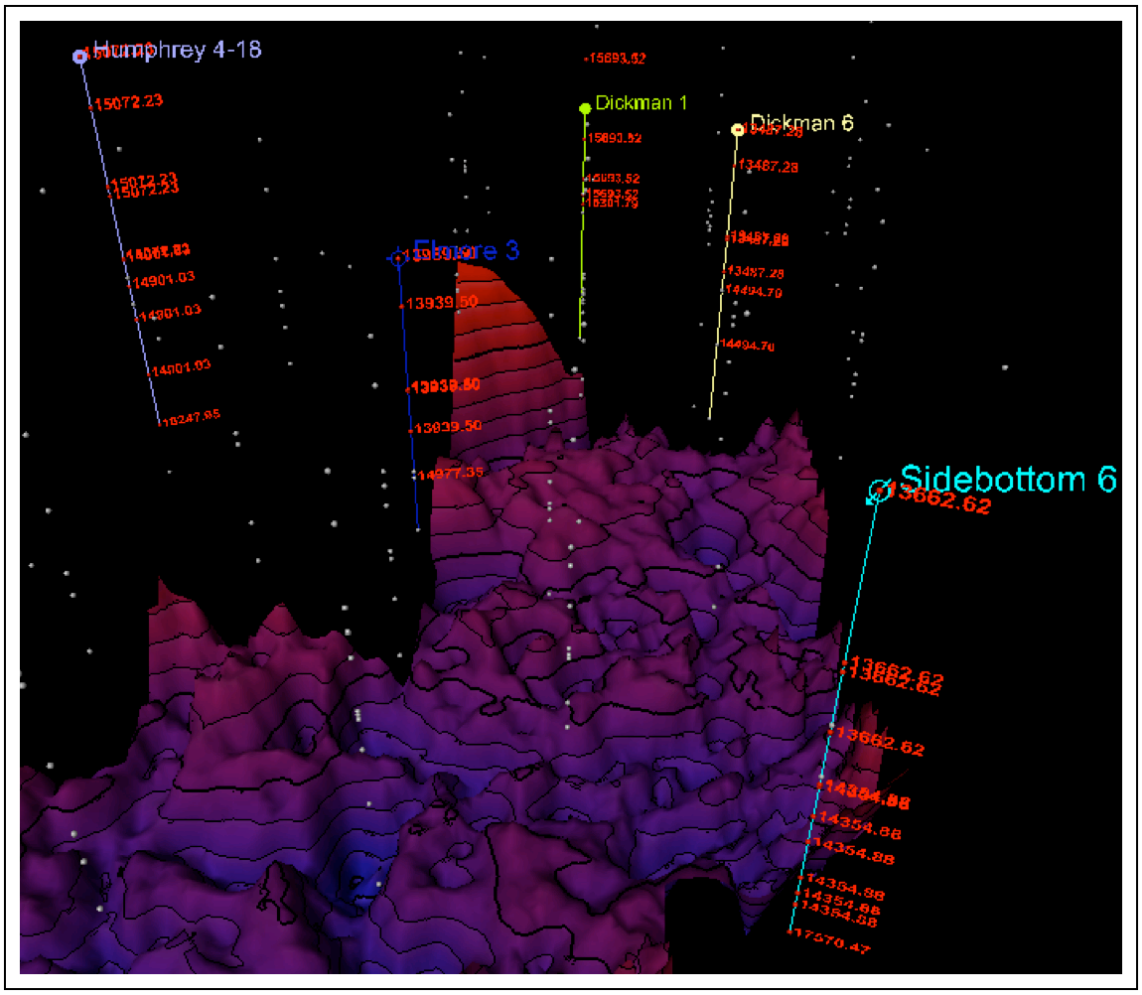

Fig.14. Zone-averaged velocity for five wells with sonic logs. The top of the 3D block is hung on Fort Scott Horizon. Vertical exaggeration 50:1 (vetical axis is time). The red-purple surface in the 3D view is the B-Zone, the bottom of the model. There are up to eight interval velocities computed based on the lithozones. The well residual time-depth curves will be corrected by these interval velocities for the next version of the velocity model.

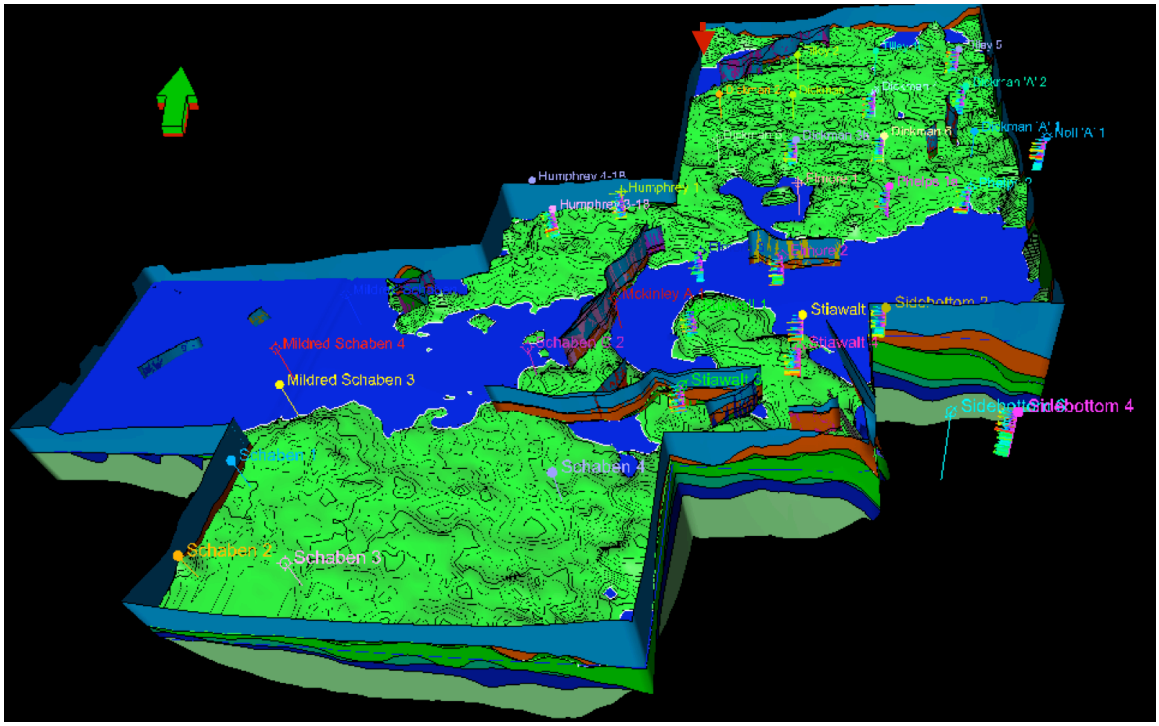

Fig. 15. Model in Depth (M3) domain ready for the CMG Grid Builder. Vertical exaggeration 50:1. Original oil water contact seen in the well data is posted for QC and reservoir volumetrics. The reservoir area is much larger than it should be. This revealed errors in T-Z conversion. To improve this conversion is a task for the next reporting period.

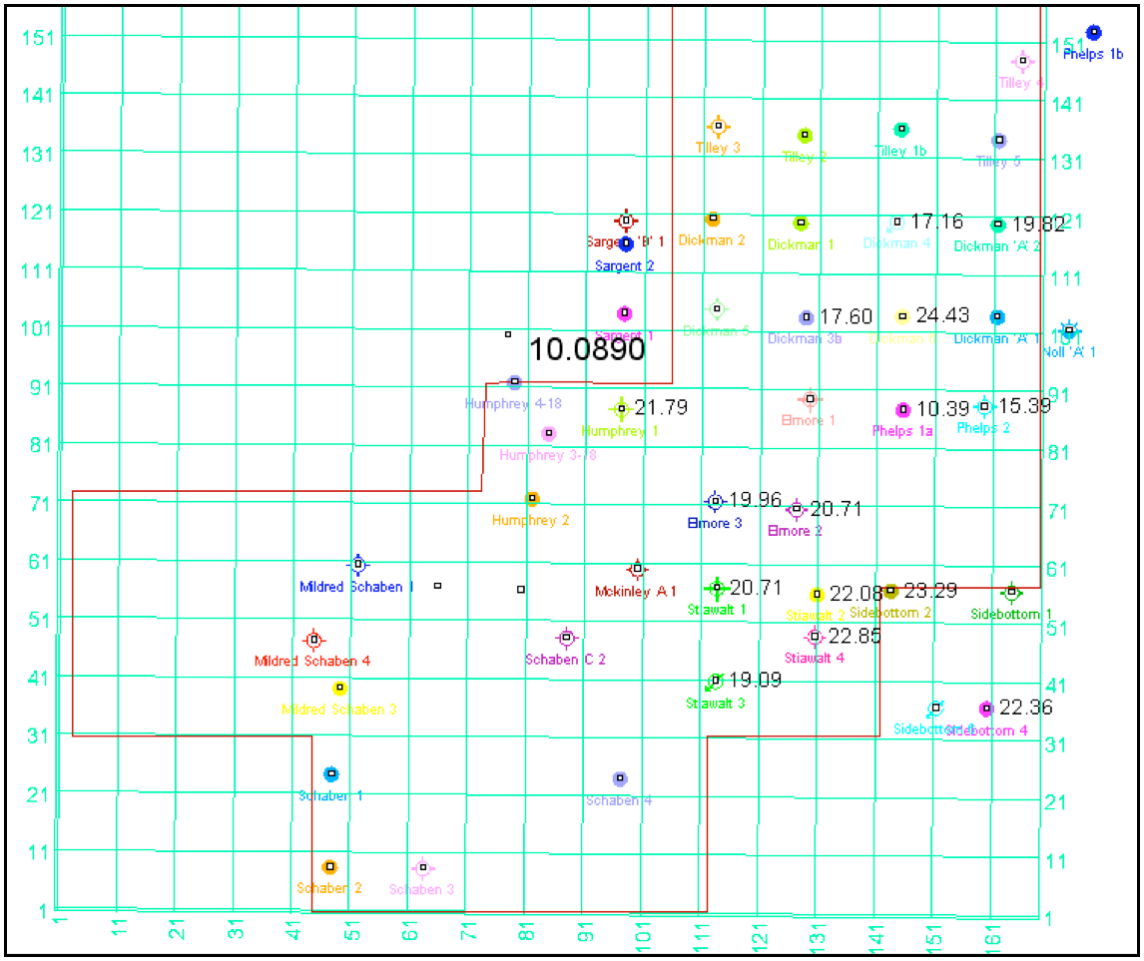

Fig. 16. A zone-average Porosity (NPHI) map for Mississippian carbonate. Number in large font is the density porosity from one well. The other values reflect estimated pure limestone porosity and well be corrected based on dolomite contents of lithozones. The corrected values will be lower than those shown in the map.

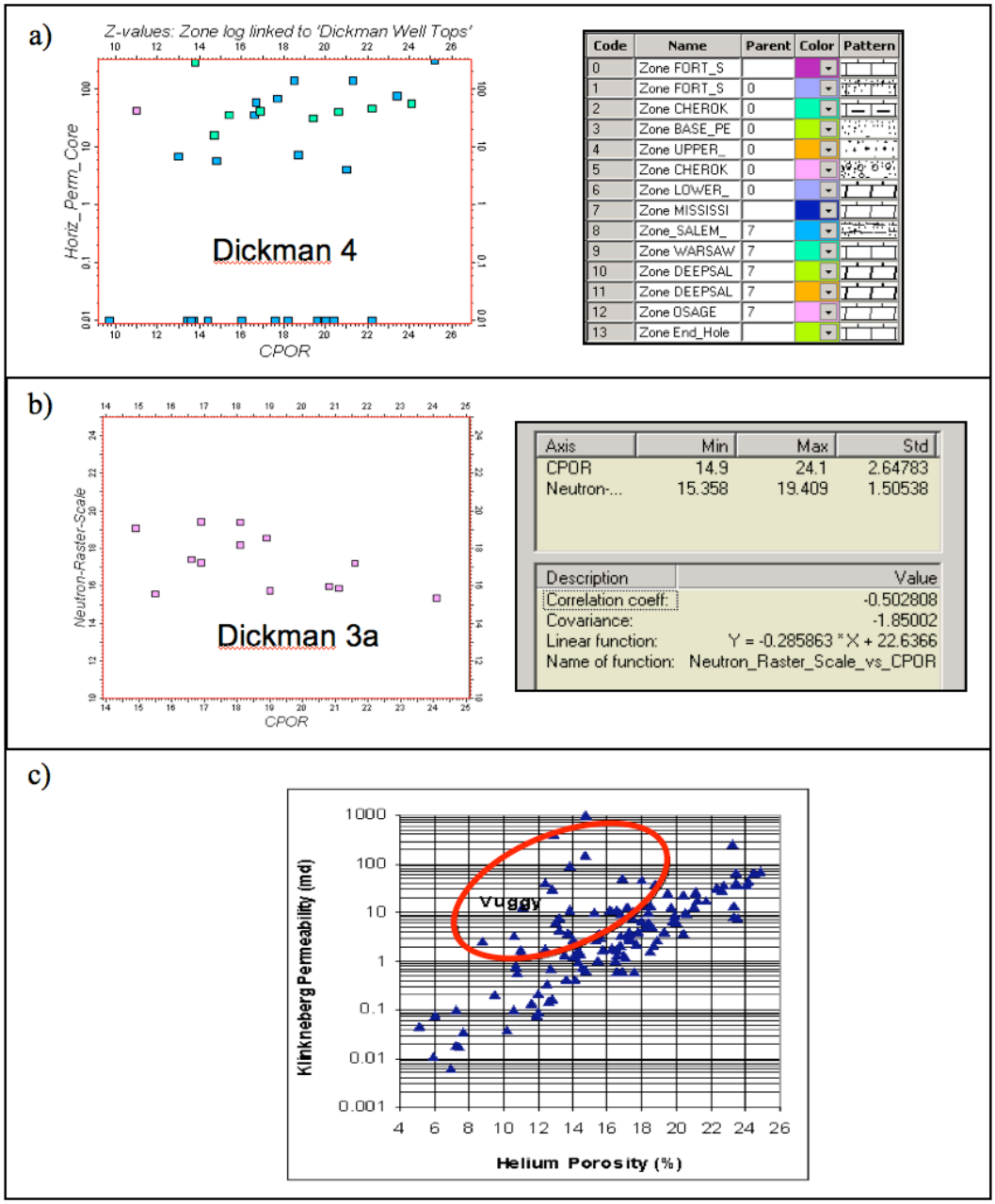

Fig. 17. Sample plots for estimating the permeability. (a) Relationship between core porosity (CPOR) and horizontal permeability (CK_h) through different zones in Dickman 4 well. The point colors in the plot correspond to lithozones Warsaw Limestone (light blue), Salem limestone (dark blue), Lower Cherokee Sandstone (pink). The CK_h to CPOR correlation is poor for Salem Limestone and is much better for the Warsaw Limestone (the reservoir). (b) Relationship between core porosity (CPOR) and log porosity (NPHI) in Dickman 3a well (correlation coefficient is - 0.5). (c) Relationship between core porosity and core permeability in Upper Osagian reservoir of the Schaben Field, a stratigraphic equivalent of the deep saline aquifer of the Dickman area.

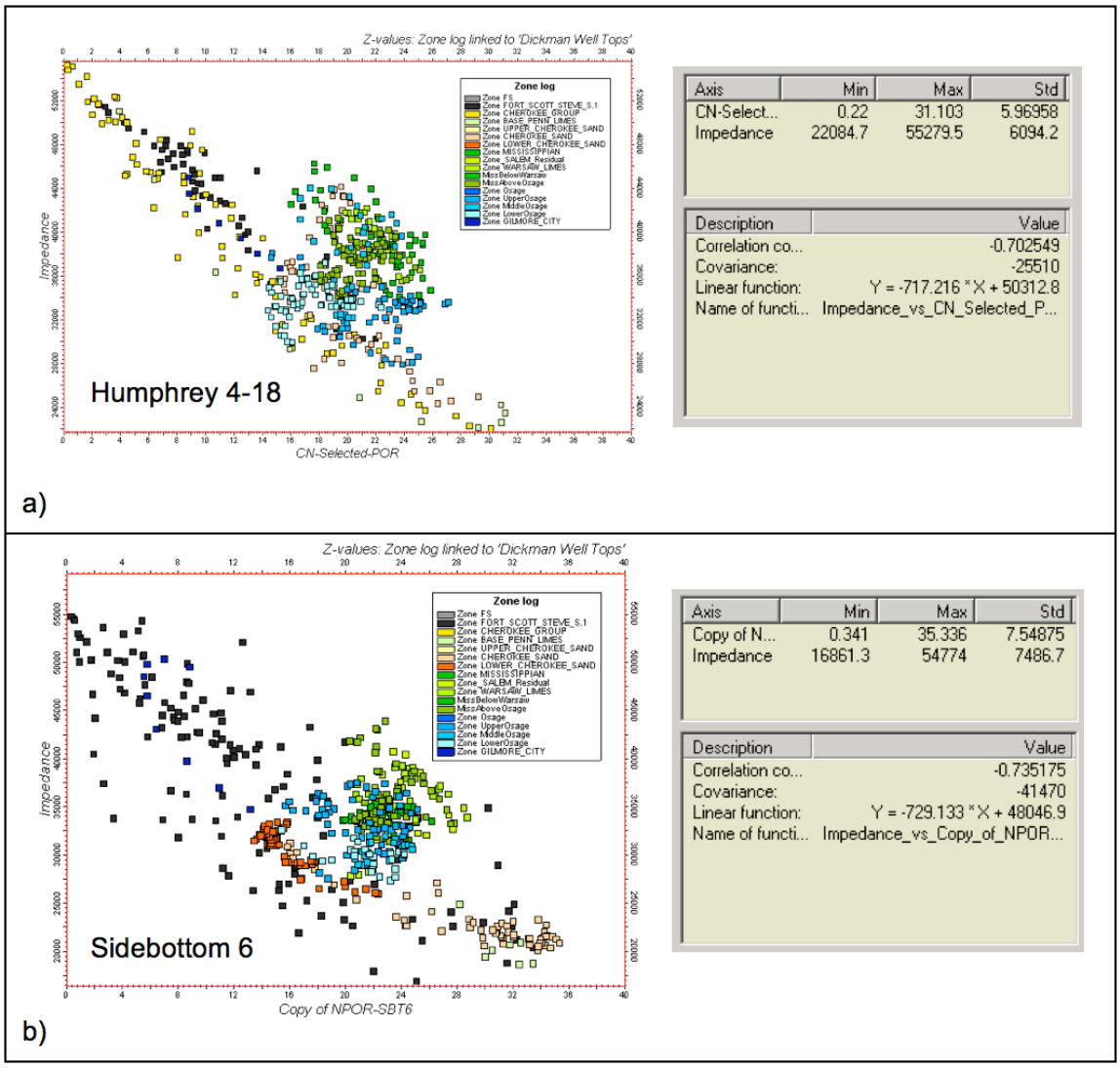

Fig. 18 Cross plots showing the relationship between neutron porosity amd impedance (RHOB*VELC) for lithozones in Fort Scott and Mississippi targets in (a) Humphrey 4-18 and (b) Sidebottom 6 wells. Point colors correspond to lithozones as indicated in the legend. The correlation coefficients are shown in the tables to the right.

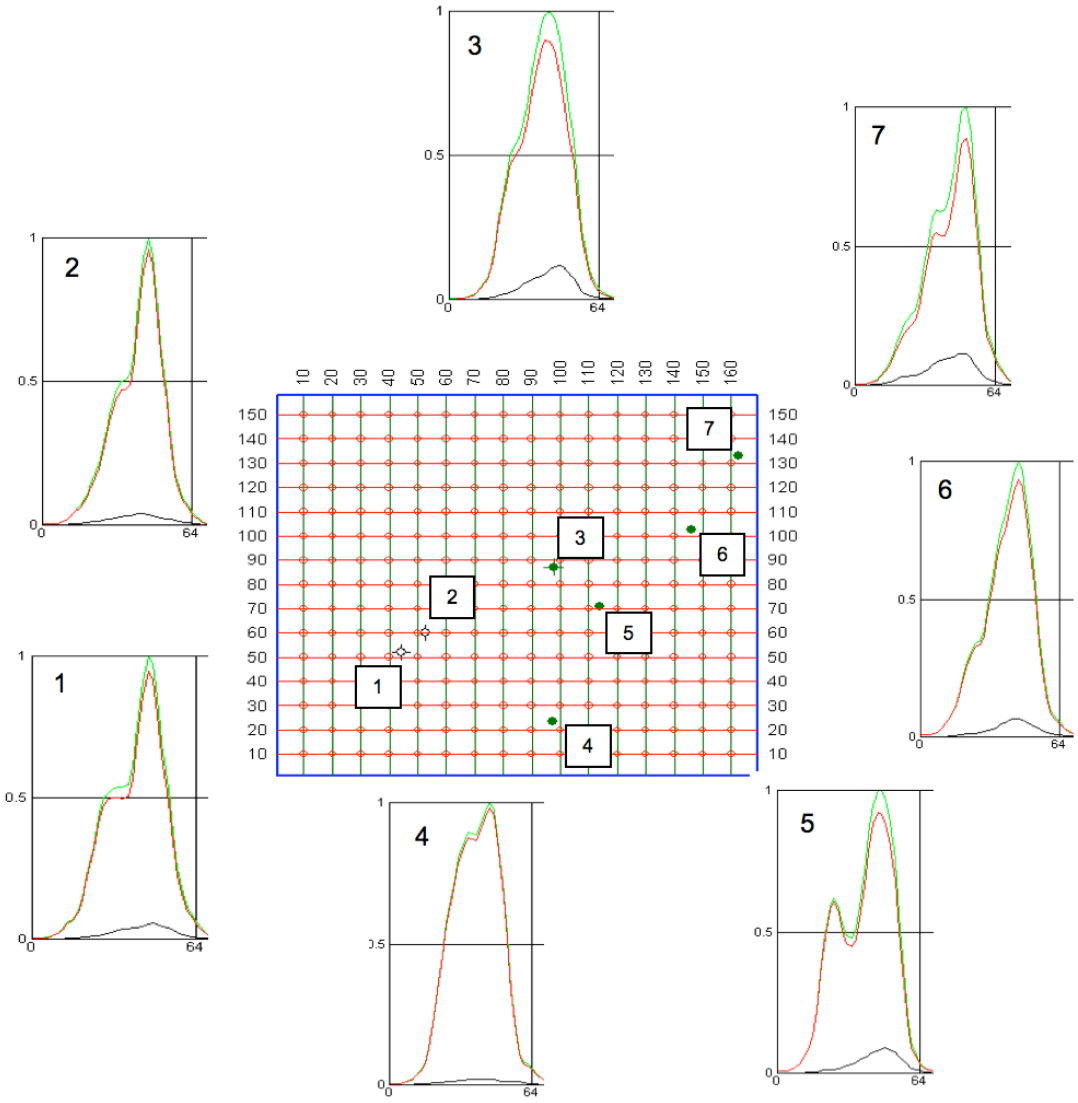

Fig. 19. The well locations for the frequency analysis (upper left) and the frequency spectra of the traces around the chosen well locations within a 500 ft radius and between 0.65 to 0.95 second.

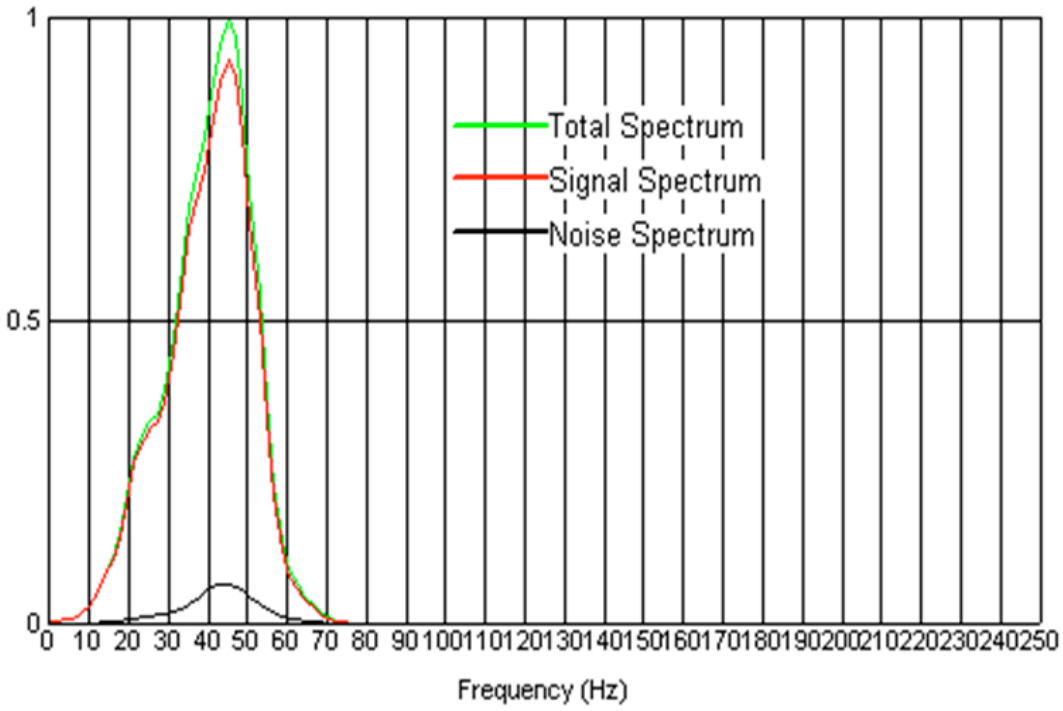

Fig. 20. The full frequency spectrum of the traces within 500 ft of the Elmore 3 well (well #5 in Figure 19).

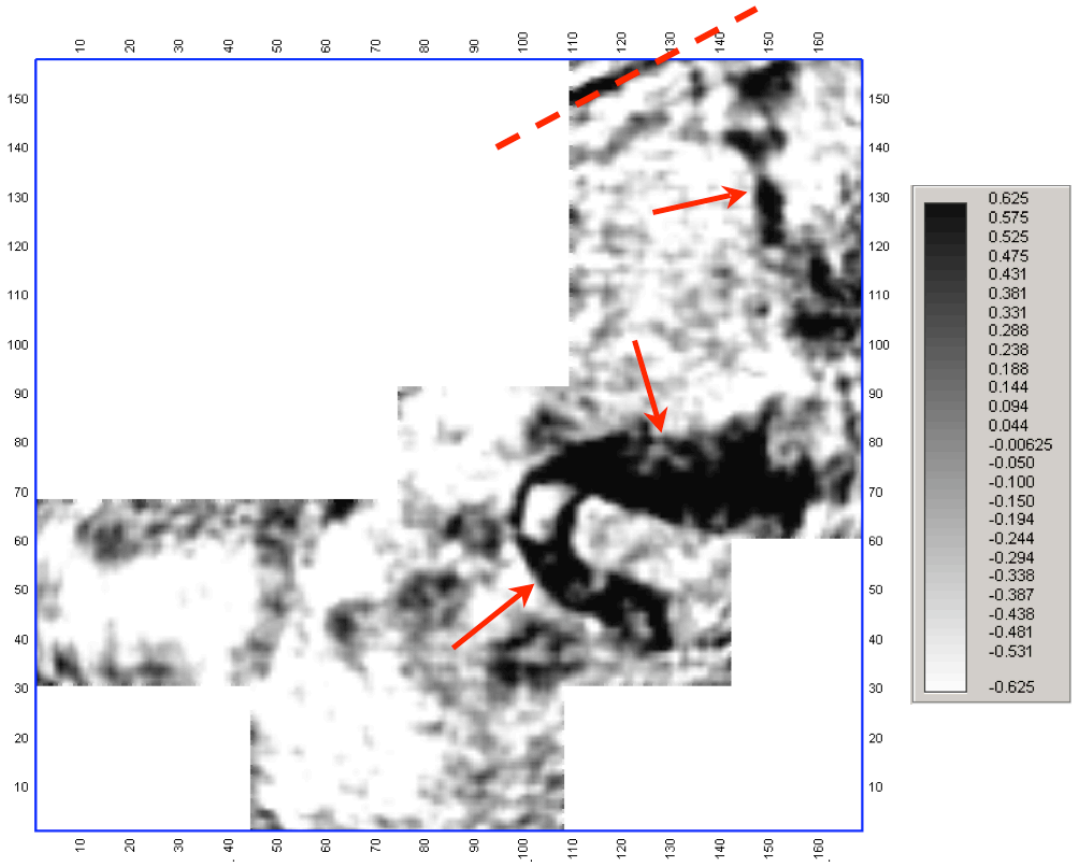

Fig. 21. Amplitude time slice at 848 ms, approximately corresponding to the top of the Mississippian. arrowed arrows indicate a channel feature incised on top of the Mississippi Unconformity and filled with Lower Cherokee sandstone. Dashed red line indicates a NE-SW trending fault.

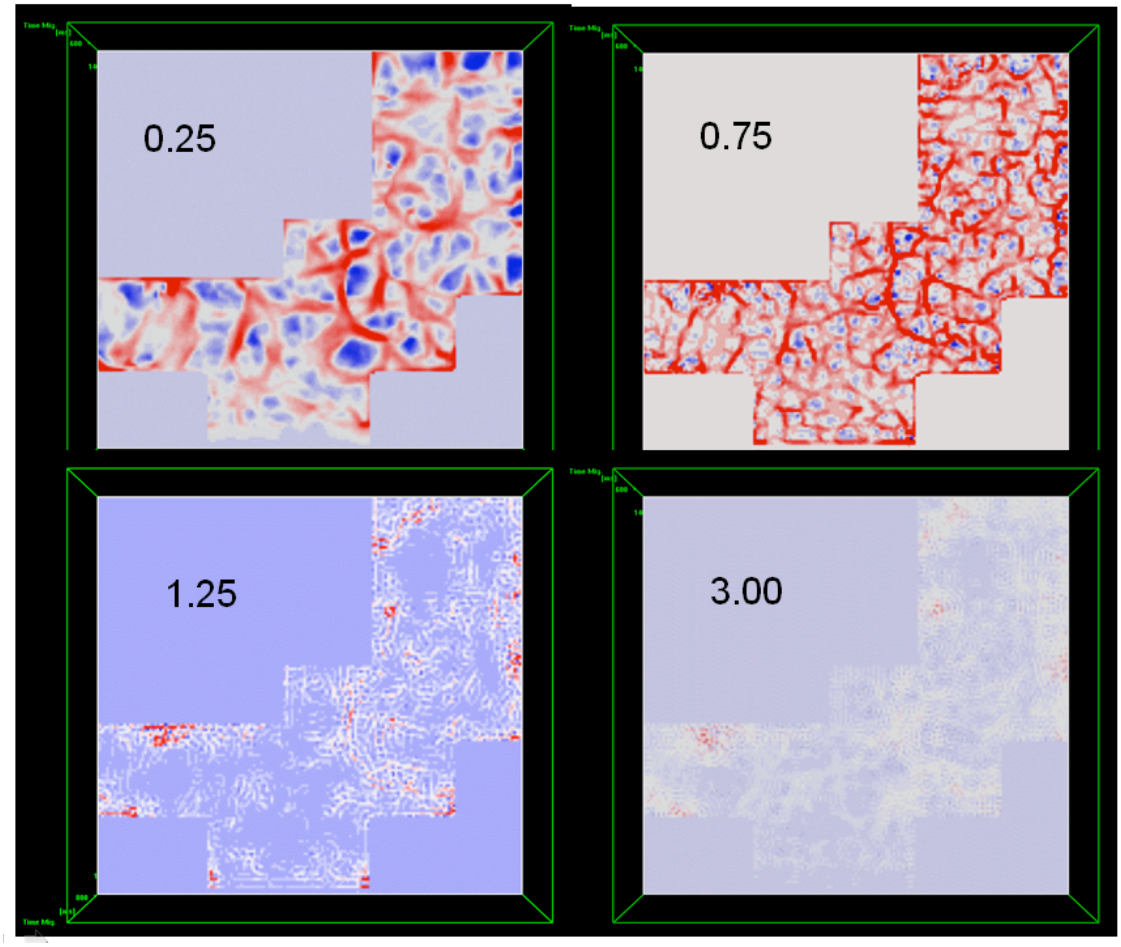

Fig. 22 Positive curvature time slices at 848ms holding all parameters constant except for power. The number listed in each image corresponds to the value of the power parameter. Based on best correlation with known features in the data, we chose 0.25 as the optimum power value.

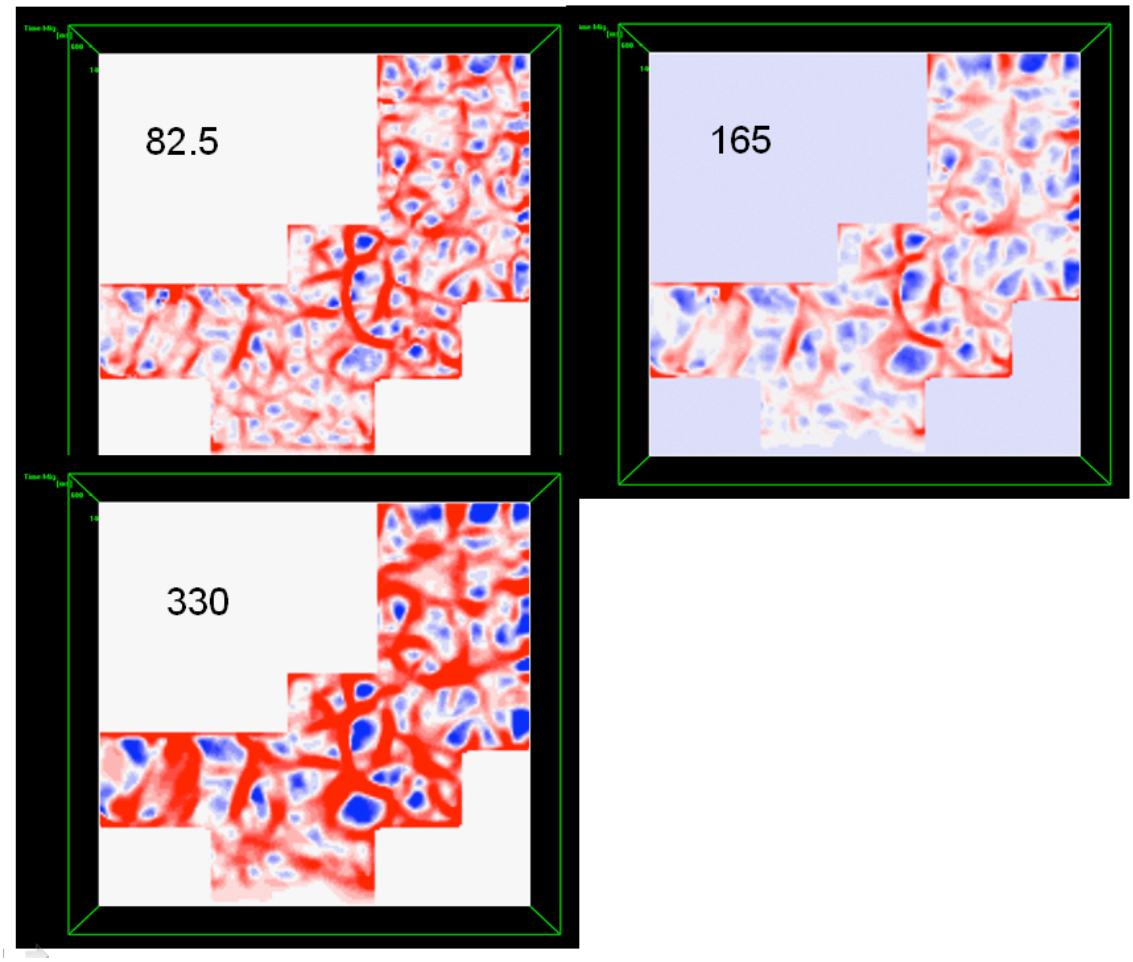

Fig. 23. Positive curvature time slices at 848ms holding all parameters constant except for the lambda parameter that relates to smoothness and average feature size. The number listed in each image corresponds to the value of the lambda parameter and we determined that 165 gave the most realistic level of complexity and correlation with known features.

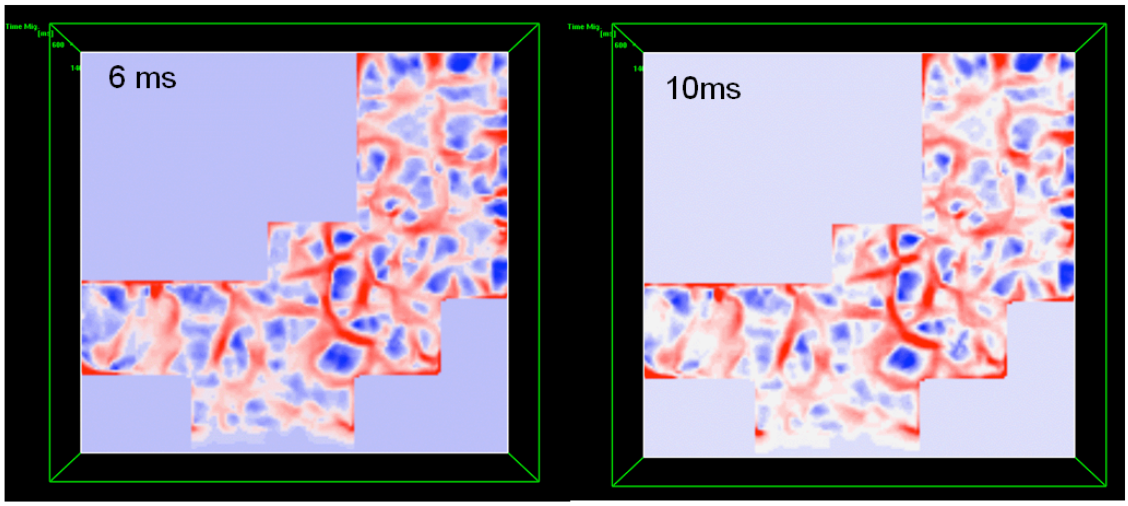

Fig. 24. Positive curvature time slices at 848ms holding all parameters constant except for time window, a parameter describing the length of the analysis window. The number listed in each image corresponds to the value of the time window in ms. The separate images are displayed with slightly different color bars. The results were not very sensitive to this parameter, but 10 ms seemed slightly better.

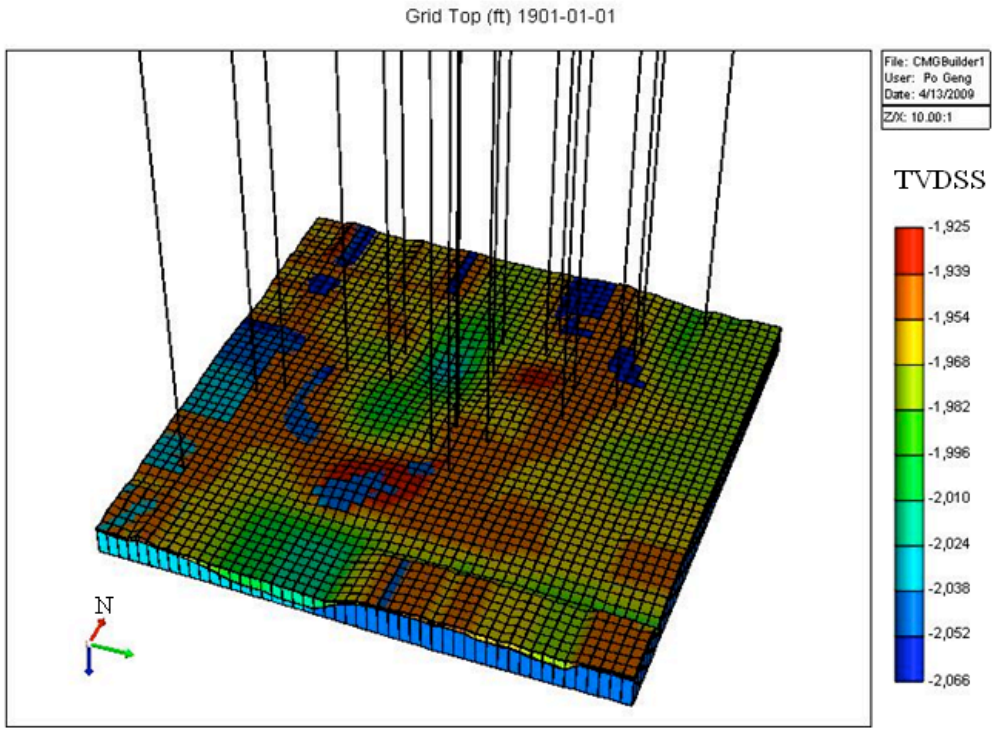

Fig. 25 A preliminary 3D simulation grid with production wells. The grid hangs on the top of Lower Cherokee Sandstone. The LC sandstone layer is in green at the front edge of the grid, and the Mississippi carbonate reservoir below is in blue. Top surface colors represent true vertical depth (subsea).